

## **Copyright Warning & Restrictions**

The copyright law of the United States (Title 17, United States Code) governs the making of photocopies or other reproductions of copyrighted material.

Under certain conditions specified in the law, libraries and archives are authorized to furnish a photocopy or other reproduction. One of these specified conditions is that the photocopy or reproduction is not to be “used for any purpose other than private study, scholarship, or research.” If a user makes a request for, or later uses, a photocopy or reproduction for purposes in excess of “fair use” that user may be liable for copyright infringement,

This institution reserves the right to refuse to accept a copying order if, in its judgment, fulfillment of the order would involve violation of copyright law.

**Please Note: The author retains the copyright while the New Jersey Institute of Technology reserves the right to distribute this thesis or dissertation**

Printing note: If you do not wish to print this page, then select “Pages from: first page # to: last page #” on the print dialog screen

The Van Houten library has removed some of the personal information and all signatures from the approval page and biographical sketches of theses and dissertations in order to protect the identity of NJIT graduates and faculty.

## INFORMATION TO USERS

This manuscript has been reproduced from the microfilm master. UMI films the text directly from the original or copy submitted. Thus, some thesis and dissertation copies are in typewriter face, while others may be from any type of computer printer.

**The quality of this reproduction is dependent upon the quality of the copy submitted.** Broken or indistinct print, colored or poor quality illustrations and photographs, print bleedthrough, substandard margins, and improper alignment can adversely affect reproduction.

In the unlikely event that the author did not send UMI a complete manuscript and there are missing pages, these will be noted. Also, if unauthorized copyright material had to be removed, a note will indicate the deletion.

Oversize materials (e.g., maps, drawings, charts) are reproduced by sectioning the original, beginning at the upper left-hand corner and continuing from left to right in equal sections with small overlaps. Each original is also photographed in one exposure and is included in reduced form at the back of the book.

Photographs included in the original manuscript have been reproduced xerographically in this copy. Higher quality 6" x 9" black and white photographic prints are available for any photographs or illustrations appearing in this copy for an additional charge. Contact UMI directly to order.

# U·M·I

University Microfilms International  
A Bell & Howell Information Company  
300 North Zeeb Road, Ann Arbor, MI 48106-1346 USA  
313/761-4700 800/521-0600

**Order Number 1356271**

**Fabrication of micron-sized mirror/cantilever silicon devices for  
crosspoint switching arrays**

**Abdel-Aziez, Yasser A., M.S.**

**New Jersey Institute of Technology, 1993**

**Copyright ©1994 by Abdel-Aziez, Yasser A. All rights reserved.**

**U·M·I**  
300 N. Zeeb Rd.  
Ann Arbor, MI 48106

## ABSTRACT

### **Fabrication of Micron-Sized Silicon Mirror/Cantilever Devices for Crosspoint Switching Arrays**

by  
Yasser A. Abdel-Aziez

This thesis describes the fabrication of micron-sized vertical mirrors at the end of horizontal cantilevers, that are electrostatically controlled. The mirrors,  $40 \times 40 \mu\text{m}$  with thicknesses of  $1.5\text{-}6 \mu\text{m}$ , were made by using the etch resistance to 40% KOH etchant of  $\langle 111 \rangle$  planes and oxide stripes. The cantilever beams, 100 to  $350 \mu\text{m}$  long and  $0.44$  to  $0.81 \mu\text{m}$  thick, were fabricated using the etch resistance of heavily doped boron layers to 10% KOH at  $50^\circ\text{C}$ . Two technologies to introduce the boron layers were investigated. The ion implantation approach was based on thick oxide/photoresist masking. A maximum doping of  $2.5 \times 10^{20} \text{cm}^{-3}$  was achieved in a layer of about  $0.83 \mu\text{m}$ . This doping level resulted in  $0.44 \mu\text{m}$  thick cantilevers after 2 hours etching to remove  $40 \mu\text{m}$  of silicon under the cantilevers. Using Spin On Doped Glass (SOG) technology, a higher doping concentration was achieved,  $5 \times 10^{20} \text{cm}^{-3}$  in a layer of  $1.9 \mu\text{m}$ . After etching 2.06 hours to remove  $26 \mu\text{m}$  of silicon, the etched cantilevers were  $0.81 \mu\text{m}$ .

Two masking methods for the SOG technique were investigated. The thick ( $40 \mu\text{m}$ ) positive photoresist method had a problem of chemical reaction between the photoresist and the spun on doped glass. The other method, which used thin negative photoresist, was more promising. Problems related to the partial etching of the mirrors due to the incomplete SOG wetting of the mirrors' sidewalls, and proximity photoresist exposure effects, can be overcome with additional experimental work.

**FABRICATION OF MICRON-SIZED  
MIRROR/CANTILEVER SILICON  
DEVICES FOR CROSSPOINT SWITCHING ARRAYS**

by  
Yasser A. Abdel-Aziz

A Thesis  
Submitted to the Faculty of  
New Jersey Institute of Technology  
in Partial Fulfillment of the Requirements for the Degree of  
Master of Science

Department of Electrical Engineering

January 1994

**Copyright © 1994 by Yasser A. Abdel-Aziz**

**ALL RIGHTS RESERVED**

**APPROVAL PAGE**

**Fabrication of Micron-Sized Mirror/Cantilever  
Silicon Devices for Crosspoint Switching Arrays**

Yasser A. Abdel-Aziez

---

Dr. Roy H. Cornely, Thesis Advisor date  
Professor of Electrical and Computer Engineering,  
NJIT.

---

Dr. Robert B. Marcus, Committee Member date  
Research Professor, Dept. of Physics; Dept. of  
Chemistry and Chemical Engineering, NJIT.

---

Dr. Edip Niver, Committee Member date  
Associate Professor, ECE Dept., NJIT.



## **BIOGRAPHICAL SKETCH**

**Author:** Yasser A. Abdel-Aziez

**Degree:** Master of Science in Electrical Engineering

**Date:** January 94

### **Undergraduate and Graduate Education**

- Master of Science in Electrical Engineering,  
New Jersey Institute of Technology, Newark, NJ, 1994
- Bachelor of Science in Electrical Engineering,  
Ain Shams University, Cairo, Egypt, 1984

**Major:** Electrical Engineering

**This thesis is dedicated to My Parents**

## ACKNOWLEDGMENT

I would like to express my appreciation to my thesis advisor Prof. Roy H. Cornely for his guidance and support, without him this thesis would not have been possible. I also would like to thank Prof. Robert B. Marcus for his guidance in both academic and processing technologies domains.

I'm grateful to the Navesink Engineering and Research Center of Bellcore, Red Bank, NJ, for providing the research environment and for funding the project. Special thanks to Murray Bowden and Bob Lehany for facilitating this opportunity to do this project. I also thank Ned Stoffel for the ion implantation processing and Tom Gmitter for the oxidation and constructive help in the spin on diffusion process. I extend my thanks to Tirunelveli S. Ravi, Jim Ringo, John Johnson for introducing me to various laboratory procedures. I'm also grateful to David D. M. Hwang for his valuable suggestions and advice. I also thank Bart Van Der Gaag for the SEM work.

Last, but certainly not least, I'm very grateful to Prof. Kosonocky and my colleagues of the Image Sensors Lab.; without their help, writing this thesis would not be possible. I appreciate my family for their patience. I also thank my friends who helped me through editing, writing, or proofreading, especially Nana Shigamatsu.

## Table of Contents

| Chapter   | Page |
|---|------|
| 1. INTRODUCTION.....  | 01   |
| 2. SILICON MICROMACHINING & LIGHT SCANNING TECHNIQUES:                            |      |
| A BACKGROUND.....   | 04   |
| 2.1. History Of Micromachining.....   | 04   |
| 2.2. Silicon Micromachining And Light Scanning Techniques.....                    | 04   |
| 2.3. Electrostatic Scanners.....  | 07   |
| 2.4. Theory Behind The Device.....  | 08   |
| 2.4.1. Electrostatic Force.....   | 08   |
| 2.4.2. Frequency Response Of The Cantilever Beam.....                             | 09   |
| 2.5. Anisotropic Etching Of Crystalline Silicon.....                              | 11   |
| 2.5.1. Orientation Dependence.....  | 12   |
| 2.5.2. Influence Of Dopants.....  | 13   |
| 2.6. Fabrication Approaches For Light Scanners.....                               | 15   |
| 2.6.1. Heavily Doped Boron Layers Grown Epitaxially.....                          | 17   |
| 2.6.2. Ion Implantation Approach.....   | 20   |
| 2.6.3. Spin On Doped Glass Approach.....  | 23   |
| 2.6.4. Expected Doping Profile In The Cantilever/Mirror Regions.....              | 23   |
| 3. FABRICATION PROCESSES.....   | 27   |
| 3.1. Introduction.....  | 27   |
| 3.2. Mirror Formation.....  | 27   |
| 3.2.1. General Procedure.....   | 28   |
| 3.2.2. Fabrication Steps.....   | 28   |
| 3.3. Cantilever Formation.....  | 31   |
| 3.3.1. Heavily Doped Layers Epitaxially Grown.....                                | 32   |
| 3.3.2. Heavily Doped Layers Introduced By Ion Implantation.....                   | 34   |
| 3.3.3. Heavily Doped Boron Layers Introduced By Spin On<br>Diffusion.....         | 37   |
| 3.4. Fabrication Of An Optical Switch.....  | 39   |
| 3.4.1. Thin Photoresist Approach.....   | 39   |
| 3.4.2. Thick Photoresist Technique.....   | 42   |
| 4. EXPERIMENTAL RESULTS.....  | 46   |
| 4.1. Introduction.....  | 46   |
| 4.2. Mirror Fabrication Results.....  | 46   |
| 4.3. Epitaxially Grown Layers results.....  | 46   |
| 4.3.1. Surface morphology results.....  | 46   |
| 4.3.2. Etching Rate Results.....  | 48   |
| 4.4. Results Of Heavily Doped Boron Layers Introduced By Ion<br>Implantation..... | 50   |
| 4.4.1. Heavily Doped P Layer Thinning And Surface Morphology.....                 | 51   |

| Chapter  | Page |
|--|------|
| 4.5. Results Of Heavily Doped Layers Introduced By Spin On Doped Glass ..... | 60   |
| 4.5.1. Heavily Doped Layer Measurements .....                                | 61   |
| 4.5.2. Cantilever Beam Fabrication Results .....                             | 62   |
| 4.6. Optical Switch Fabrication Results .....                                | 62   |
| 4.6.1. Positive PR AZ 4620-E Technique Results.....                          | 63   |
| 4.6.2. Negative PR AZ 5214 Technique Results.....                            | 65   |
| 4.7 Surface Smoothing Experimental Results.....                              | 67   |
| 5. DISCUSSION OF EXPERIMENTAL RESULTS.....                                   | 69   |
| 5.1. Introduction .....  | 69   |
| 5.2. Heavily Doped Layers Epitaxially Grown .....                            | 69   |
| 5.3. Heavily Doped Layers Introduced By Ion Implantation.....                | 70   |
| 5.3.1. P++ Layer Etching.....  | 70   |
| 5.3.2. Ion Implantation Masking Effects.....                                 | 70   |
| 5.3.3. Mechanical Stresses Effects Due To High Doping Concentration .....    | 71   |
| 5.3.4. Inward Versus Downward <110> Etching Rates .....                      | 73   |
| 5.3.5. Problems Associated With Ion Implantation .....                       | 73   |
| 5.4. Heavily Doped Layers Introduced By Spin On Glass (SOG).....             | 74   |
| 5.4.1. Etching Rate Of P++ Regions And Masking Effects .....                 | 74   |
| 5.5. Device Fabrication.....   | 75   |
| 5.5.1. Positive Thick Photoresist Approach.....                              | 75   |
| 5.5.2. Negative Thin Photoresist Approach .....                              | 75   |
| 5.5.2.1 Mirror Thinning .....  | 76   |
| 5.5.2.2. Cantilever Beam Separation From The Mirror .....                    | 77   |
| 5.6. Effect Of Adding Alcohol To The Etchants .....                          | 78   |
| 6. SUMMARY AND CONCLUSION.....   | 79   |
| APPENDIX A.....  | 81   |
| BIBLIOGRAPHY .....   | 82   |

PLEASE NOTE

Page(s) missing in number only; text follows.  
Filmed as received.

ix  
x  
xi  
xii  
xiii

University Microfilms International

| <b>List of figures</b>   | <b>Page</b> |
|--|-------------|
| 1.1 A 22 optical switch array. ....  | 2           |
| 2.1 A basic design for a high inertia reflective scanner(4). ....  | 6           |
| 2.2 A basic design for low inertia optical scanner that depends on changing the index of refraction using electric field(4). ....  | 6           |
| 2.3 A basic design for an electrostatic optical switch (4) ....  | 7           |
| 2.4 A cantilever beam dimensions and its axis used for frequency response studying(4). ....  | 9           |
| 2.5 Extrapolated data from ref. (2) showing the relative etch rate for <100> Si vs. KOH concentration at different boron doping levels. ....   | 16          |
| 2.6 <100> silicon etch rate as a function of the boron concentration for various KOH solutions at a temperature of 60 °C. ....   | 16          |
| 2.7 A layout of the basic processing steps to fabricate an optical switch using heavily doped boron layers epitaxially grown. ....   | 18          |
| 2.8 A layout of the basic mirror formation steps. ....   | 21          |
| 2.9 A layout of the basic fabrication steps of an optical switch using ion implantation to introduce heavily doped boron layer. ....   | 22          |
| 2.10 A basic layout of processing step to fabricate an optical switch by introducing a heavily doped boron layer using spin on doped glass. ....   | 24          |
| 2.11 A figure that shows the expected doping profile of boron in the cantilever/mirror regions. In (a) and (b), the sideview and the plan are shown. While the cross section A-A' shows the boron profile in the hatched area, which will depend on the boron diffusivity. Also, section B-B' shows that some boron atoms may not diffuse through the entire mirror thickness and the region beneath it. In (e), the cross section of the expected cantilever/mirror regions after etching is shown. Notice the thickness variations under the mirror due to less doping concentration. .... | 25          |
| 3.1 Normal <111> planes to <110> planes in <110> orientation silicon(4). ....  | 28          |
| 3.2 Etched hexagonal holes in alignment region of the silicon wafer made using 50 mm diameters circular holes in oxide mask. Marker A, B and C show the edges of the vertical and non vertical <111> planes and photoresist lines, respectively. The lines were aligned parallel to the vertical <111> edges and were formed using alignment region of mask 2. ....  | 30          |
| 3.3 The pattern used to form cantilever beams. ....  | 31          |
| 3.4 The doping profile of sample (1) of an epi grown layer. The maximum doping concentration was $5 \times 10^{19} \text{ cm}^{-3}$ . ....   | 32          |
| 3.5 The doping profile of sample (2) of an epi grown layer. The maximum doping concentration was $9 \times 10^{19} \text{ cm}^{-3}$ . ....   | 33          |
| 3.6 The doping profile of sample (3) of an epi grown layer. The maximum doping was $10^{20} \text{ cm}^{-3}$ . ....  | 33          |
| 3.7 A basic layout of a cantilever beam formation by using ion implantation to introduce heavily doped boron layer. ....   | 35          |
| 3.8 A layout of a cantilever beam formation using etch stop layer introduced by spin on doped glass. ....  | 38          |

|           |   |    |
|-----------|---|----|
| 3.9       | A layout of the fabrication steps of an optical switch using thin negative photoresist AZ 5214.....   | 41 |
| 3.10      | A cross section of the mask and the sample shows their relative positions during the exposure step to transfer the cantilever pattern to the oxide mask to fabricate an optical switch.....   | 42 |
| 3.11      | A layout of the fabrication steps of an optical switch using thick positive photoresist AZ 4620-E.....  | 43 |
| 3.12      | A cross section shows the relative positions of the mask and the sample during the exposure step to transfer the cantilever pattern to the oxide mask using thin negative AZ PR 5214.....   | 45 |
| 4.1       | SEM micrograph for an etched mirror in 40% KOH solution for 2 hours followed by 5 minutes of etching in (40% KOH + 25% Isopropyl alcohol) solution at 50 °C. a) A sideview, and b) a front view of the mirror.....  | 47 |
| 4.2       | A top view (a) and side view (b) of an etched epi grown layer of heavily doped boron relative to an oxide mask. It is clear the cause of the different etch rates of the white (heavy doped p) and the gray (high density point defects) regions. ....  | 48 |
| 4.3       | The etched depth versus time for the sample of doping profile shown in fig (3.4).....   | 49 |
| 4.4       | The etched depth versus time for the sample of doping profile shown in fig (3.5).....   | 49 |
| 4.5       | The etched depth versus time for the sample of doping profile shown in fig (3.6).....   | 50 |
| 4.6.a,b   | A SEM micrographs show the etching results of cantilever beams introduced by ion implantation. This sample etched in 10% KOH at 50 oC. In a), a raw of cantilever beams is shown. Notice the broken cantilever side in the side of the cantilever.....  | 52 |
| 4.6.c,d,e | In c), a 0.44 mm thick cantilever beam after 2 hours etching is shown. In d), a micrograph shows a 100 mm cantilever beam sticking to the sample surface while the close up shows clearly the broken side of the post. In e), a trace of the etched planes. Notice the insert of a hexahedral etched hole <sup>(6)</sup> in <110> wafer for comparison.....   | 53 |
| 4.7       | The optical micrographs of a sample received 1.5 doses of ion implantation. Notice the thin texture of the boron layer and the jagged edges of the pattern. Also, notice the black dots scattered on the pattern (a). The high magnification in (b) shows a black dot as a valley, marker B, while marker A is pointing at etched plane in the first stages of the etching. Also, marker C is pointing at the corner (inward) etching in the post's region (c)..... | 55 |
| 4.8       | The etching curve of the previous sample in fig.(4.7).....  | 56 |
| 4.9       | The optical micrograph of a sample received 2.5 doses of ion implantation shows sharp edges and firm texture for the cantilever beam pattern. Notice the straight 100 μm long cantilever beam. ....   | 56 |
| 4.10      | The etching curve for the pervious sample, fig. (4.9).....  | 57 |



|         |   |    |
|---------|---|----|
| 4.11    | The optical micrograph of the sample received 2.5 doses of ion implantation. Notice the firm texture of the boron layer and the markers A and B are pointing at the etched planes and the post edge respectively (a). While, an etched part of the post is shown in (b). Also, the crack in the brom layer was shown in about 5% of the pattern.....  | 57 |
| 4.12    | The etched curve for the previous sample, in fig. (4.11). .....   | 58 |
| 4.13    | The optical micro graph for a sample received 2.5 doses of implantation. It had PR AZ 5214 mask only. Notice the marker A for the etched planes in. Also, in this sample the cantilever beams were twisted in a spiral shape.....   | 58 |
| 4.14    | The etching curve for the previous sample fig. (4.13). .....  | 59 |
| 4.15    | A trace of the measured inward versus downward <110> etching rates. ....  | 59 |
| 4.16    | The etching results of the inward etching of the post's acute angle side versus downward <110> etching. ....  | 60 |
| 4.17    | The etching results of the inward (obtuse angle side of the post) versus downward <110> etching rates. ....   | 61 |
| 4.18    | The etching results of a cantilever pattern fabricated by spin on doped glass technology. In (a), notice the white and gray regions with zero and 4 mm etched step respectively. In (b), the etched step was 26 mm after 2.06 hours of etching in etching in 10% KOH at 50 °C. The sharp pattern definition is evident.....   | 63 |
| 4.19    | SEM micrographs for a cantilever beam fabricated by SOG. In (a), the top view of 100 mm long cantilever is shown with some curl up. In (b), a micrograph shows the non uniformity of the etched surface beside the curl of the cantilever beam. In (c), the thickness of a cantilever beam fabricated by SOG technology after 2.06 hours of etching in 10% KOH at 50 °C was 0.81 μm.....                      | 64 |
| 4.20    | A cross section of the mirror after the spinning and development of the positive PR AZ 4620-E.....  | 65 |
| 4.21    | A cross section shows an incomplete development of the sample processed with cured SOG + PR AZ 4620. ....   | 65 |
| 4.22    | SEM micrographs for optical switch fabrication results which was done by using SOG technology and negative PR AZ 5214. Notice the incomplete etching of Si beneath the cantilever, (a). Also, notice that the unprotected regions of the mirror with SOG was etched. Also, the nonuniformity of etched Si surface is shown. In (b), a close up for the enetched regions shows a uniform mirror thickness..... | 66 |
| 4.23    | A graph of the cantilever beam fabricated by thin PR Technique after etching shows the separation of the cantilever beam and the mirror around the mirror base due to proximity effects. ....   | 67 |
| 4.24.a, | A cross section of a <110> Si etched surface shows the surface roughness before using Isopropyl KOH solution.....   | 68 |
| 4.24.b, | A cross section of the above sample shows the rounded peaks of the <331> planes. This sample etched for one hour in Isopropyl KOH solution at 40 °C. Notice the unchange in the peaks' heights or the distance between them .....   | 68 |

|        |  |    |
|--------|--|----|
| 5.1.a, | A graph shows the required thickness of heavily doped layers to fabricate 1 $\mu\text{m}$ thick cantilever beams versus the etch rates of these layers.....  | 71 |
| 5.1.b, | A graph shows the measured etch rates of p++ layers at different doping concentrations versus the predicted ones.....  | 72 |
| 5.2    | A cross section in the oxide + PR mask shows the tapering effects of the mask in ion implantation technique. ....  | 72 |
| 5.3    | A cross section of a sample in which PR AZ 4620-E used to transfer the cantilever pattern. Notice that the mirror's top is covered by about 3 mm of PR, while the undeveloped parts of the sample are covered by 5-6 mm of PR. This will results in etching parts of the mirror's height in case of using RIE to etch the PR + SOG ..... | 75 |
| 5.4    | A comparison between exposure step with and without mirrors to transfer the cantilever pattern to the oxide mask using thin negative PR.....   | 77 |

**List of Tables**

**Page**

1.1 Etching rates, of different crystallographic orientation Si, and SiO<sub>2</sub>.....13

## CHAPTER (1)

### INTRODUCTION

This thesis investigated the formation of three dimensional microstructures of single crystal silicon using wet etching techniques. The emphasis was on forming a cantilever beam device to be used as the moving arm of an optically smooth micromirror that can deflect a light beam in the wafer plane. An array of such devices would be used as optical switches. The work reported was done with Dr. R. H. Cornely of the ECE Dept. of NJIT, Newark, NJ and Dr. R. B. Marcus at the Navesink Engineering Research Center of Bellcore, Red Bank, NJ.

This research was the second phase of the optical switch project done at Bellcore, Red Bank, NJ. The first phase was to fabricate optically smooth vertical micromirrors. The results of this research work were published in 1992 <sup>(1)</sup>. The second phase of the research was based on utilizing the etch stop properties of heavily doped boron layer <sup>(2)</sup> to form a cantilever beam attached to a post on which the reflecting mirror was held. See fig. (1.1), which shows a  $2 \times 2$  array of cantilever/mirror devices.

Single crystal silicon micromachining is an emerging technology that implements standard processes techniques for integrated circuits to fabricate three dimensional novel structures. This technology has been used in the past decade to fabricate ink jet nozzles, pressure sensors, speedometers and optical switches <sup>(3)</sup>, <sup>(4)</sup>.

Light scanning techniques have been reported using torosional mirrors that reflect the light beam normal to the wafer plane using silicon dioxide <sup>(3)</sup>, <sup>(4)</sup>. Some applications as an optical voltmeter and four channel optical multiplexer were discussed in publications in 1988 <sup>(4)</sup>. The new design of the authors <sup>(1)</sup> was aimed at reflecting the light beam in the wafer plane. This would allow a crosspoint array to be fabricated.

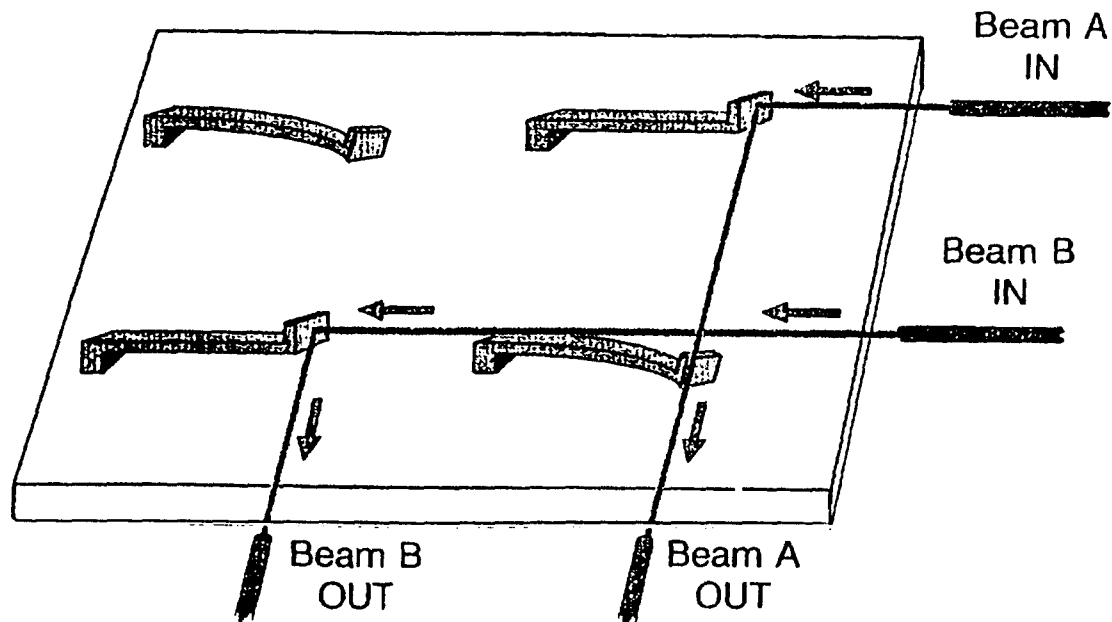


**Figure 1.1** A  $2 \times 2$  optical switch array.

The design has the potential to make low insertion loss crosspoint array. The research in this thesis had two objectives:

- 1) Investigate the different process techniques for forming a heavily doped boron layer; This layer can serve as an etch stop layer from which the cantilever beam could be fabricated ;
- 2) The fabrication of a  $2 \times 2$  array of electrostatically movable micromirrors using the boron doping technology most compatible with the mirror fabrication processing.

Chapter (2) gives a short review of the history of micromachining and movable optical mirror techniques. Some emphasis is given to the theory of the electrostatic forces acting on the cantilever beams and the characteristic of the motion of such beams. Also, the theoretical models and some results of recently published research on the etch stop behavior of crystalline silicon in alkaline solutions are given so that the reader will

be able to follow the etching research reported in this work. A review of possible ways to fabricate the mirror cantilever switch is presented.

In chapter (3), the detailed experimental steps used in this work are given with detailed figures for each step. Most of the fabrication work was done to prepare heavily doped boron layers so that the etch stop behavior of these  $p^{++}$  layers could be studied. However some other experiments were not carried out, e.g. the epitaxial growth approach, because of cost considerations and the preliminary results that dictated improvement of the quality of highly doped epi layers which would require major research effort. The ion implantation work was also terminated because of the cost, mainly machine time, involved in making doping level above  $10^{20} \text{ cm}^{-3}$ , which was too low for obtaining the required low etch rates. The third approach, which appeared most promising, was the spin on glass (SOG) technique. The thick photolithography approach developed a problem with chemical reaction between the photoresist and doped glass that prevented a complete photoresist development. The other approach, which involve oxidation and thin photoresist, had a problem due to the proximity effect associated with photoresist exposure, due to the 40 micron high mirrors seperating the mask for the photoresist. In chapter (4), the experimental results for each process will be presented. Problems and other findings will be discussed in detail in chapter (5).

Finally, chapter (6) will give a summary of the results and suggestions for future research.

## CHAPTER (2)

### SILICON MICROMACHINING & LIGHT SCANNING TECHNIQUES

#### A BACKGROUND

##### 2.1. History Of Micromachining

Silicon, the second most abundant element in the earth's crust (26%), has been regarded just as important for inorganic chemistry as carbon for organic and it could be considered man's most useful element.

Micromechanics as a silicon based device technology was actually initiated by H. C. Nathanson *et al* <sup>(5)</sup> at WESTINGHOUSE RESEARCH LABORATORIES in 1965 when he & R. H. Wickstrom introduced the Resonant Gate Transistor. Because of practical problems, such as reproducibility, temperature stability and limitation on life time due to fatigue, RGT's have never been realized. But in 1975 an important technical achievement was made at the INTEGRATED CIRCUIT LABORATORY at STANFORD UNIVERSITY. It was a complete Gas Chromatograph integrated on a 2" wafer, and this demonstrated the possibility to integrate sensors, mechanical elements and electronic devices on small areas (volumes). This can be considered the birth of micromechanics. Micromechanics has been defined as the technology aimed at the construction of micronsized mechanical structures that are tested to perform electrical and mechanical functions. Examples are, pressure sensors, accelerometers, nozzles and optical switches. As Stefan Johnasson quoted <sup>(5)</sup> " An optimistic opinion is that the field of Micromechanics will become of the same importance as microelectronics ".

##### 2.2. Silicon Micromachining And Light Scanning Techniques

The excellent mechanical properties of single crystal silicon <sup>(1), (5)</sup> led to the growing interest in using it in micromechanics to develop batch fabricated, inexpensive and high

performance sensors and actuators using IC fabrication techniques. One can summarize the reasons for Si success in micromachining as:

- 1) Well established technologies with high precision, batch fabrication and reproducibility;
- 2) High performance mechanical properties because of the high purity and low defect density ;
- 3) Easy to integrate with electronic circuits.

Light scanning applications for silicon in micromechanics provided a background that led to this thesis work. Light Scanning can be divided into two groups

#### **A) High Inertia Scanners**

In this type of scanners a reflective device like mirrors is mounted on the axis of high speed motors to deflect the light beam in certain direction. These scanners have high deflection angle ( $360^\circ$ ) and high frequency of 50,000 rpm, see fig. (2.1).

#### **B) Low Inertia Scanners**

This type of scanners can be divided according to the way the light is been handled into

##### **1) Refractive**

In this type of scanners, changing the index of refraction using electric field or acoustic waves, one can change the direction of light, see fig. (2.2).

##### **2) Reflective**

In this type of scanners a reflective light element such as mirrors is mounted on a vibrating element that allows the mirror to reflect the light beam. The vibrating element



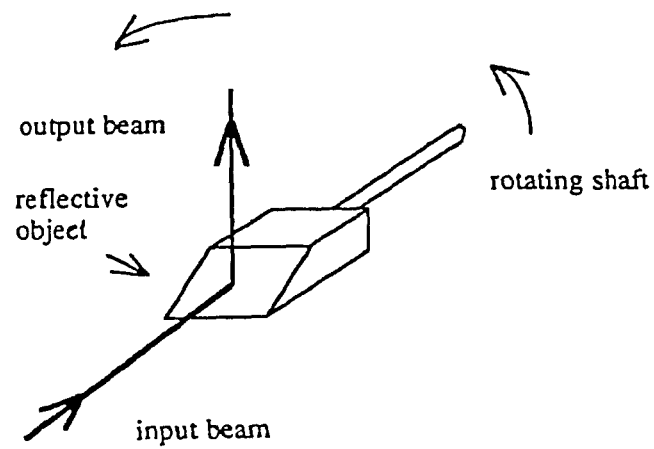


**Figure 2.1** A basic design for a high inertia reflective scanner<sup>(4)</sup>.

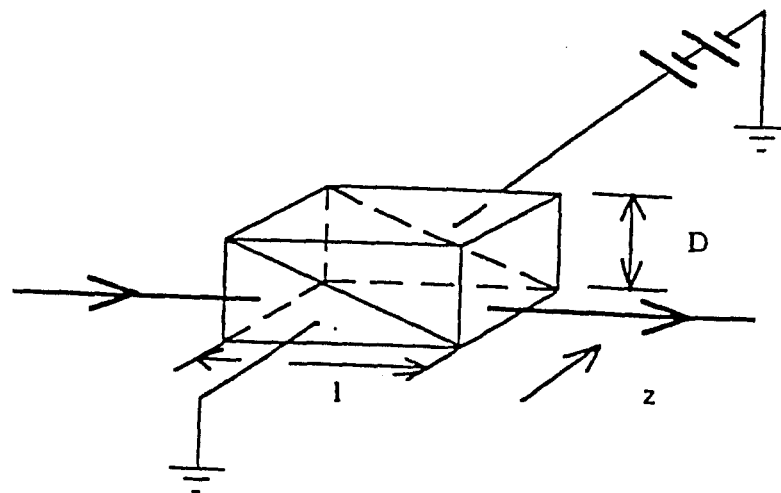


**Figure 2.2** A basic design for low inertia optical scanner that depends on changing the index of refraction using electric field<sup>(4)</sup>.

can be moved by electrostatic force, electromagnetic field or piezoelectric effects. Fig (2.3) shows a basic design to an electrostatic optical switch (4).

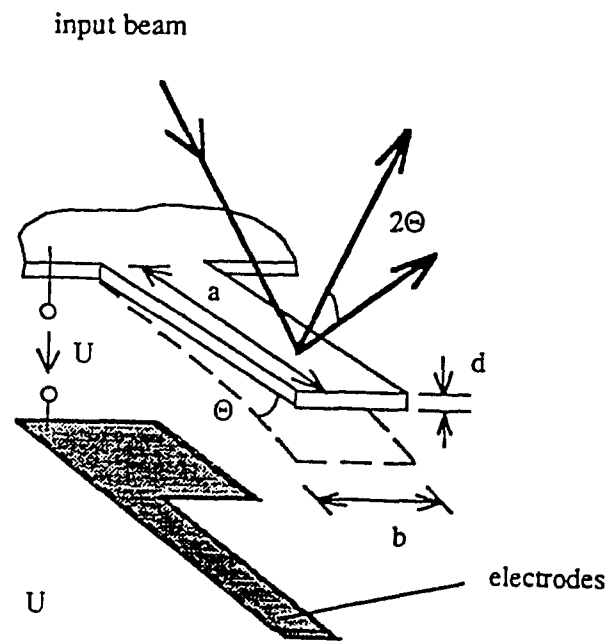


Figure 2.3 A basic design for an electrostatic optical switch (4)

### 2.3. Electrostatic Scanners

Peterson first introduced a new class of scanners in 1977 & 1980 when he published a work in micromechanical light modulator of silicon dioxide on a silicon torsional mirrors<sup>(3)</sup>. This class of scanners relies on electrostatic attraction and accordingly utilize coulomb force as a motive force to excite the mirror into motion. A research by K. Gustfsson in 1988 published his results on a fiber optic switch, which a four channel fiber optic multiplexer and a novel fiber optic voltmeter applying electrostatic and electromagnetic principles (4).

In all previous light scanning device the incident beam and reflected light were normal to the wafer plane which can be considered to be an obstacle for integration of the switch with a system and gives a good chance for increasing insertion loss. Review fig. (2.3).

The approach to light deflection studied in this research was to reflect the light beam in the wafer plane by mounting the scanning mirror on an electrostatically movable cantilever. The advantage of this approach is that the light switch can be controlled individually to reflect the light beam between two certain points without interference with any other switch. See fig. (1.1)

## 2.4. Theory Behind The Device

### 2.4.1. Electrostatic Force

As mentioned in the previous section that the optical switch utilizes the electrostatic attractive force to move the mirror. An approximate expression for the small deflection angle  $\Theta$  of a cantilever beam at its tip under the influence of electrostatic attraction force is (4)

$$\Theta \cong \frac{\epsilon}{E} \frac{1}{d_o^2} [a/d]^3 U^2 \quad (2.1)$$

Where:

- $\theta$  is the angular deflection
- $\epsilon$  is the material permittivity
- $E$  is Young's modules
- $d_o$  is the separation between the cantilever beam and electrode
- $U$  is the applied voltage

To achieve high enough electrostatic force on the cantilever beams, the electrode separation must be in the  $\mu\text{m}$  range. The moment of inertia of the beam must be low enough for the forces acting on the beam to induce enough bending (deflection) on the beam, that is the thickness of the beam must be small. Since the quality factor  $Q$  of the silicon is as high as 3000 much greater deflection angles can be achieved by operating the cantilever at reduced pressure.

#### 2.4.2. Frequency Response Of The Cantilever Beam

In section (2.4.1) the relation between cantilever different parameters, the applied voltage and the angular deflection shows that the that cantilever dimension must be in the  $\mu\text{m}$  range. As a matter of fact a miniaturization of the switches or sensors in general will have the following advantages:

- a) Faster response, and less influence by the sensor on the measuring object;
- b) New accessible measurements ;
- c) Integration of the sensors with other electronic elements to fabricate smart sensors ;
- d) Higher reliability by minimizing the number of connections ;
- e) Batchfabrication which reduces costs.

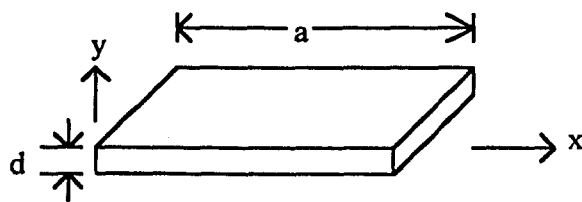


Figure 2.4 A cantilever beam dimensions and its axis used for frequency response studying<sup>(4)</sup>.

Fig (2.4) shows a part of a cantilever beam have been used to study the frequency response. The fundamental frequency for the cantilever beam is given by (4)

$$f_o = 0.162 \frac{d}{a^2} \left[ \frac{E}{\rho} \right]^{1/2} \quad (2.2)$$

Where

- E is Young's Modules
- $\rho$  is the density of the material

when the beam is subject to bending, there is a net variation in its surface area, the relative change  $\Delta A/A$  is

$$\Delta A/A = -2\nu\varepsilon^2 \quad (2.3)$$

Where

- $\nu$  is Possion's ratio
- $\varepsilon$  is the surface strain which is a function of the axial coordinates, x , along the length of the beam.

The total area of variation can be calculated as  $\Delta A/A$

$$\Delta A/A = -2\nu \int_0^a \varepsilon^2 dx \quad (2.4)$$

In the fundamental resonance mode,  $\varepsilon$  is well approximated by a second order polynomial. The area variation calculated will cause the surface energy of the bent beam to be somewhat altered and thus affecting the resonance frequency. The coefficient of energy shift is  $\sigma_s$

$$\Delta U = \sigma_s \Delta A \quad (2.5)$$

According to the Rayleigh method for the resonance frequency calculations, the fundamental resonance frequency is determined by equating the maximum potential and kinetic energies is

$$f_r = f_o \left(1 - 12 \sigma_s \frac{v}{Ed}\right)^{1/2} \quad (2.6)$$

In semiconductor materials  $\sigma_s$  is normally  $0.8-1.8 \text{ Jm}^{-2}$  where E is in the order of  $10^{12} \text{ N/m}^2$ . It is clear that the surface energy will only be significant when the beam thickness d approaches atomic dimensions, which is different than what was calculated before.

Also the calculation of the quality factor Q is more difficult because it is been affected by the rise to energy loss and hence decreasing its value. Energy loss is due to:

- 1) Acoustic radiations.
- 2) Viscous drag forces of the surrounding gas
- 3) Internal friction of the beam material itself.

Kari Gustafsson results was in agreement with continuum mechanics up to submicrometer range of cantilever thicknesses.

### 2.5. Anisotropic Etching Of Crystalline Silicon

To form an optical switch, one can use anisotropic etching. Anisotropic etching of crystalline silicon have been studied by many authors (1), (3), (4), (6), (7) & (8). The anisotropic etching phenomenon can be referred to:

- 1) The crystalline orientation by which one can form vertical deep U structures of  $\langle 110 \rangle$  orientation wafers or V grooves using  $\langle 100 \rangle$  orientation wafers.
- 2) High doping concentration of boron reduces the etch rate inversely to the fourth power of that concentration (4).

An article published by Seidel and his colleagues in 1990 consisted of two parts to study the anisotropic phenomenon for crystal orientation dependence and the influence of doping (4). In the following sections, a summary of their findings and a theoretical model proposed by them will be presented.

### **2.5.1. Orientation Dependence**

An electrochemical model proposed describing the anisotropic etching behavior of different crystal planes in all alkaline solutions. In this model, "in an oxidation step, four hydroxide ions react with one surface silicon atom, leading to the injection of four electrons into the conduction band. These electrons stay localized near the crystal surface due to the presence of space charge layer. The reaction is accompanied by the breaking of the backbonds, which require the thermal excitation of the perspective surface state electrons into the conduction band. This step is considered to be rate limiting. In the reduction step, the injected electrons reacts with water molecules to form new hydroxide ion and hydrogen. It is assumed that these hydroxide ions generated at the surface are consumed in the oxidation reaction rather than those from the bulk electrolyte, since the latter are kept away from the crystal by repellent force of negative surface charge. According to this model, monosilicic acid  $\text{Si}(\text{OH})_4$  is formed as the primary dissolution product in all anisotropic silicon etchants. The anisotropic behavior is due to small differences of the energy level of backbond surface state as a function of crystal orientation"(2).

Table (1.1) summarize the experimental results of the etching rate of crystal orientations and some passivation layers published by Clarck and Edell <sup>(10)</sup>. These results used as a reference through this research.

It is clear from the table the difference in etching rates for different planes can give a higher aspect ratios of  $\langle 110 \rangle / \langle 111 \rangle$  and  $\langle 110 \rangle / \text{SiO}_2$  to be used in micronsized structures. Another important point in the Seidel results, is that addition of 25% of isopropyl alcohol to 20% KOH solution will reduce the etching rate by 20% of the  $\langle 100 \rangle$  planes, while for  $\langle 110 \rangle$  the planes the reduction will be 90%.

### 2.5.2. Influence Of Dopants

The second part of the Seidel article dealt with the effect of the boron doping concentration level on etching rates.

**Table 1.1** Etching rates of different crystallographic orientation of Si and SiO<sub>2</sub>.

| Wt. pct. of KOH flakes in H <sub>2</sub> O. | True KOH wt. pct. % | Temp. °C | $\langle 110 \rangle$ Si $\mu\text{m/hr}$ | $\langle 111 \rangle$ Si $\mu\text{m/hr}$ | SiO <sub>2</sub> $\text{\AA/hr}$ | $\langle 110 \rangle \div \langle 111 \rangle$ | $\langle 110 \rangle \div \text{SiO}_2$ |
|---|---------------------|----------|---|---|----------------------------------|--|---|
| 10  | 9                   | 23       | 0.49                                      | 0.13                                      | 5.3                              | 3.8  | 920                                     |
| 10  | 9                   | 40       | 4.6                                       | 0.49                                      | 37                               | 9.4  | 1200                                    |
| 10  | 9                   | 50-      | 19  | 0.85                                      | 0.99                             | 22   | 1900                                    |
| 10  | 9                   | 80       | 100                                       | 3.1                                       | 100                              | 32   | 910                                     |
| 30  | 27                  | 23       | 2.8                                       | 0.07                                      | 9.7                              | 40   | 2900                                    |
| 30  | 27                  | 40       | 10  | 0.24                                      | 48                               | 42   | 2100                                    |
| 30  | 27                  | 50       | 24  | 0.29                                      | 180                              | 83   | 1300                                    |
| 30  | 27                  | 80       | 130                                       | 0.93                                      | 2100                             | 140  | 680                                     |
| 40  | 36                  | 23       | 2.3                                       | 0.031                                     | 9.9                              | 74   | 2300                                    |
| 40  | 36                  | 40       | 9   | 0.094                                     | 51                               | 96   | 1800                                    |
| 40  | 36                  | 50       | 22  | 0.15                                      | 130                              | 150  | 1700                                    |
| 40  | 36                  | 80       | 120                                       | 0.69                                      | 2100                             | 170  | 570                                     |
| 50  | 45                  | 23       | 1.2                                       | 0.007                                     | 11                               | 160  | 1100                                    |
| 50  | 45                  | 40       | 4.4                                       | 0.026                                     | 55                               | 17   | 800                                     |
| 50  | 45                  | 50       | 10  | 0.062                                     | 180                              | 160  | 560                                     |
| 50  | 45                  | 80       | 87  | 0.48                                      | 1900                             | 180  | 460                                     |



The following are direct quotations from his publication describing the etch stop phenomena. "The article describes the critical concentration  $C_0$  below which the etching rate is independent of the boron concentration and equal to  $R_i$  (initial etch rate). Two relations were introduced. The first was the etch rate dependence on the doping concentration

$$R = \frac{R_i}{[1 + (C_B/C_0)^a]^{4/a}} \quad (2.7)$$

Where (a) is  $>0$  and determines the smoothness of the transition region around  $C_0$ . The second relation was the temperature dependence of the etch rate and the doping concentration

$$R(T) = \frac{R_0 C_0'^4}{C_B^4} e^{-(E_1 + 4E_2)/KT} \quad (2.8)$$

The above relation is valid for  $C_B > C_0$ .

where

$$R_i(T) = R_0 e^{-E_1/KT}$$

$$C_0(T) = C_0' e^{-E_2/KT}$$

$E_1$  and  $E_2$  are the activation energies for the etching and doping respectively. For higher concentration, the etch rate should increase by four times the activation energy of the critical boron concentration".

"It was found for a doping concentration higher than  $2 \times 10^{19} \text{ cm}^{-3}$ , a strong reduction in etching rates. The reduction found to be inversely proportional to the fourth power of the boron concentration. For a given high boron concentrations, the etch stop effect was to be most effective at low KOH concentrations and least effective for the highly concentrated KOH. The model proposed in the article attributed the etch stop behavior to the electrical effects of holes rather than the chemical effects of boron. Due to the high dopant concentration, the width of the space charge layer on the silicon surface shrinks drastically. Therefore, electrons injected into the conduction band by an oxidation reaction cannot be confined to the surface and rapidly recombine with holes from the valence band. The lack of these electrons impedes the reduction of water and thereby the formation of new hydroxide ions at the silicon surface. Since the transfer of four electrons is required for the dissolution of one silicon atom, the observed fourth power for the decrease of the etch rate can be explained".

Extrapolated data from the article are plotted in fig.(2.5) to show the relation between the relative etch rate and the KOH concentration at different doping levels. Also, some results of the same reference are shown in fig. (2.6).

## **2.6. Fabrication Approaches For Light Scanners**

Making a cantilever system, one can use the etch resistance of the set of  $\langle 111 \rangle$  planes as well as the etch resistance of heavily doped boron. Since the geometry of the device dictates that one etch resist region must be normal and another horizontal, see fig. (1.1), one can use etch resist by crystallographic orientation to make the vertical mirror using  $\langle 110 \rangle$  material. However since  $\langle 111 \rangle$  planes are not perpendicular to each other <sup>(6)</sup>, it is not possible to use them as an etch stop for the horizontal cantilever fabrication. After making mirrors, the etch stop of heavily doped p regions must be used to make the horizontal cantilevers.

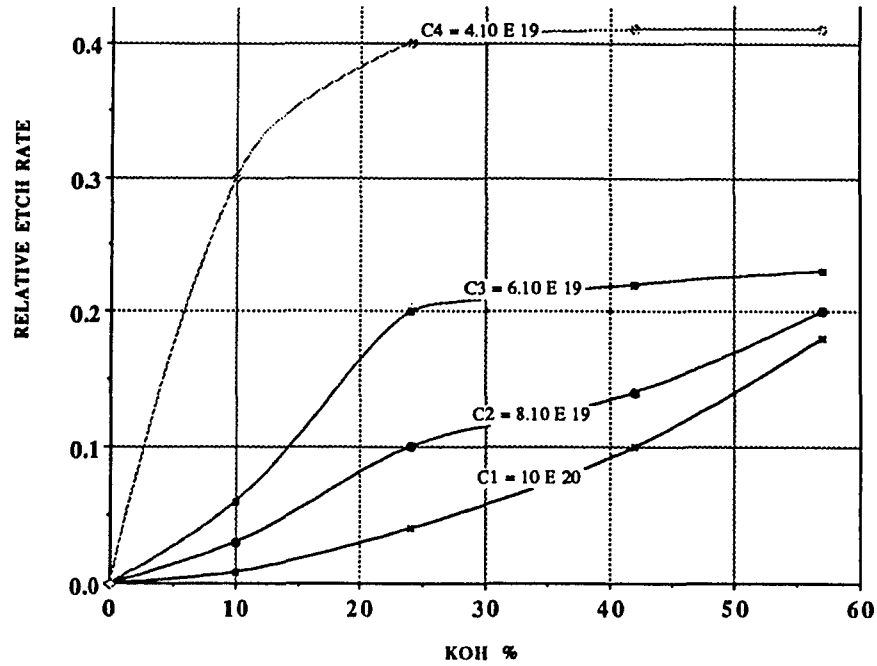


Figure 2.5 Extrapolated data from ref. (2) showing the relative etch rate for  $\langle 100 \rangle$  Si vs. KOH concentration at different boron doping levels.

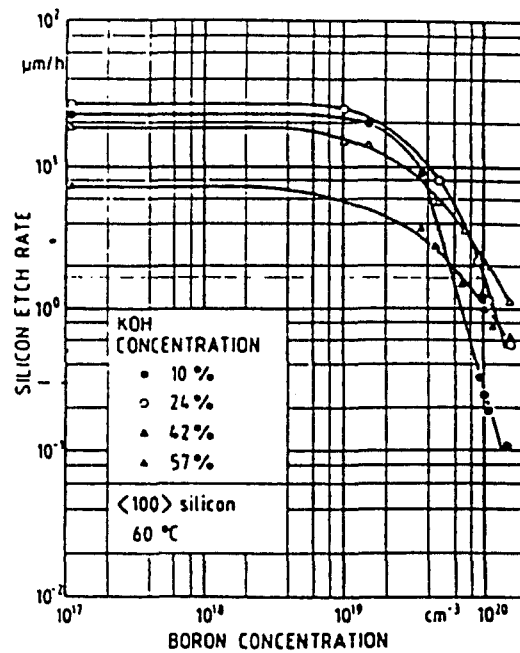


Figure 2.6  $\langle 100 \rangle$  silicon etch rate as a function of the boron concentration for various KOH solutions at a temperature of  $60^\circ\text{C}$ .

To achieve the goal of fabricating an optical switch, one must fabricate the vertical mirror first; then in a second step, the horizontal cantilever is fabricated. Optically smooth mirrors were previously fabricated <sup>(1)</sup>. The following technologies were investigated as means to introduce the heavily doped boron layers:

- 1) Epitaxial growth ;
- 2) Ion implantation ;
- 3) Spin on diffusion.

### 2.6.1. Heavily Doped Boron Layers Grown Epitaxially

In 89' Dr. R. Cornely<sup>(11)</sup> attempted to fabricate the optical switch using the etch resistance of heavily doped p layer sandwiched between heavily doped  $n^+$  layers surrounded by lightly doped p or n layers. All these layers will be epitaxially grown by Chemical Vapor Deposition (CVD).

The major fabrication steps are shown in fig. (2.7) and are as follow

#### A) Epi-layer growth

- The first layer is n with thickness equal to the desired distance from the cantilever to the substrate.
- The middle. layer is a heavily doped  $p^{++}$  of the desired cantilever thickness.
- The top layer is of whatever doping is best for obtaining low defect layer. The mirror will be formed of this layer with thickness of 30-40  $\mu\text{m}$ .

Because of these layers are grown at 800-900  $^{\circ}\text{C}$ , the boron atoms in the cantilever regions will diffuse out of the middle region when the top layer is grown. To counter this problem,  $n^{++}$  layers are grown on either side of the  $p^{++}$  so that effective thickness of the  $p^{++}$  will be of acceptable thickness for the cantilever. The epitaxial layers were grown by SPIRE CORP. on a "best effort" program. Problems encountered during the experimental fabrication research phase.

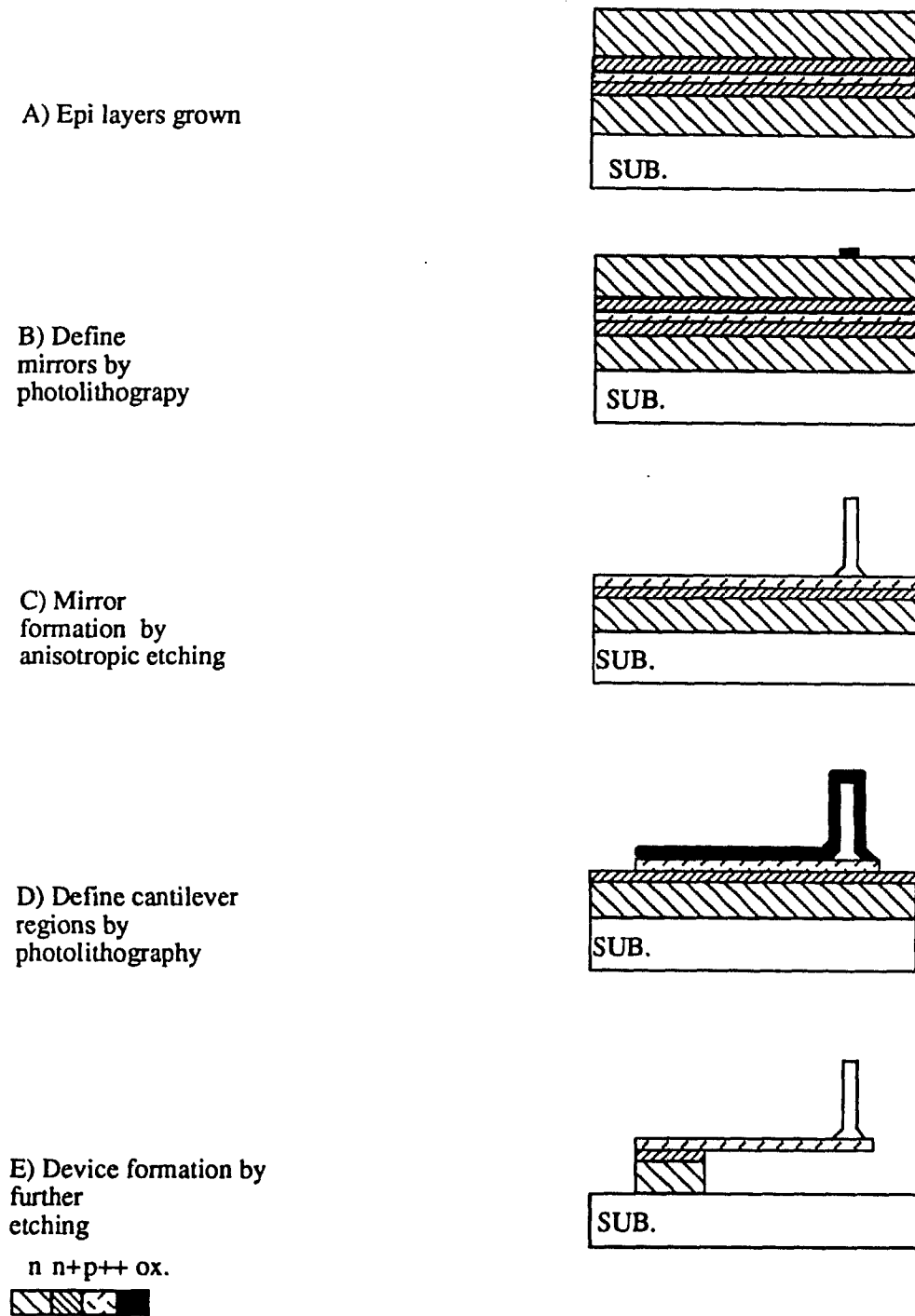


**Figure 2.7** A layout of the basic processing steps to fabricate an optical switch using heavily doped boron layers epitaxially grown.

**B) Define the mirrors**

- 1) Deposit  $\text{SiO}_2$  with the desired thickness .
- 2) Define the mirrors regions using positive photoresist, then etch the oxide except where the mirrors are.

**C) Mirrors Formation**

Using  $\text{KOH} : \text{H}_2\text{O}$  solution, etch down to reach the desired mirror height.

**D) Define Cantilever Regions**

- 1) Deposit  $\text{SiO}_2$  over the sample with the desired thickness.
- 2) Pattern the cantilever regions using positive photoresist where the cantilever are to be; then use Reactive Ion Etching to etch away the oxide else where.

Notice that you can use a thick photoresist instead of  $\text{SiO}_2$  to pattern the sample which will save one step.

**E) Device Formation**

Use  $\text{KOH}:\text{H}_2\text{O}$  solution at a suitable temperature to form the cantilevers and thus the final device.

The advantage of this process is that one can obtain ideal epitaxial layers and processing steps are relatively simple. The requirement from the research at Bellcore showed that there are serious difficulties such as

- 1) Epi layer defects arise especially when growing a 35-40  $\mu\text{m}$  thick layer. Point defects normally will not affect the mechanical cantilever properties, but the etch resistance will be lost.
- 2) Research in growing thick layers using CVD may result in layers of sufficient better quality; however, such program require several dedicated epitaxial growth systems. And this would lead to expensive manufacturing costs.

More promising approaches to form the etch stop regions for the cantilever appeared to be either ion implantation or spin on doped glass technologies.

### **2.6.2 Ion Implantation Approach**

Fig. (2.8) and (2.9) show the basic fabrication steps for the mirror and the optical switch using ion implantation technology to introduce the heavily doped boron layer. These steps are summarized in the figures and in the following sections A, B and C

#### **A) Mirror Formation**

- 1) Oxidize the sample thermally in dry oxygen to form a suitable thick oxide to protect the tops of the mirror when etching with anisotropic etchant KOH.
- 2) Define the mirror pattern using positive photoresist.
- 3) Etch the sample using KOH:H<sub>2</sub>O solution to form mirrors.

#### **B) Form Etch Stop Layer**

- 1) Oxidize the sample using wet oxidation to grow thick oxide mask against ion implantation.
- 2) Define the cantilever regions using negative photoresist.
- 3) Use ion implantation to introduce dopant into the sample with the right concentration.
- 4) Anneal the sample at fixed temperature to activate the dopant.
- 5) etch the oxide mask.

#### **C) Cantilevers Formation**

Using KOH etching, form the cantilevers.

A) Sample oxidation .

B) Transfer the circular pattern to the sample by positive PR. Then etch the oxide mask.

C) Etch hexahedral shapes by KOH etching.

D) Define mirrors by using positive PR. This done by allignment to the vertical  $\langle 111 \rangle$  plane.

E) Etch all oxide except where the mirrors will be.

F) Form mirrors by KOH etching.

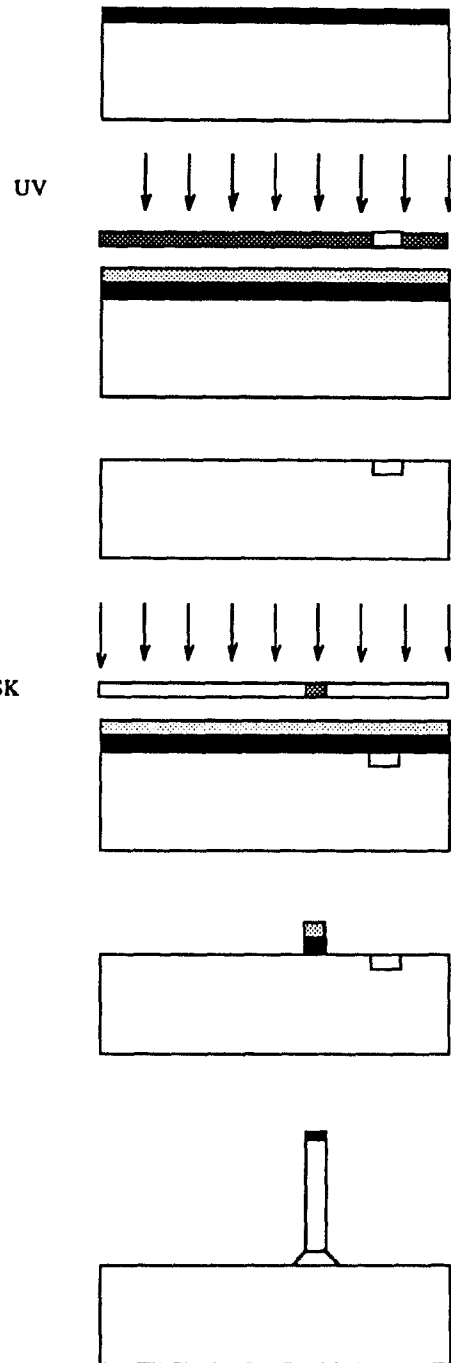
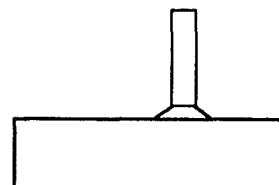


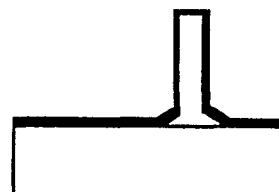
Figure 2.8 A layout of the basic mirror formation steps.



A) Form mirrors by anisotropic etching.

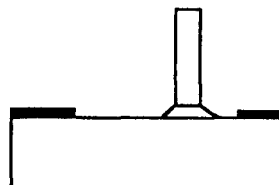


B Form oxide mask by wet oxidation.

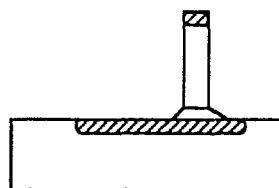


C) Form cantilever pattern by photolithography, then form heavily doped regions by ion implantation.

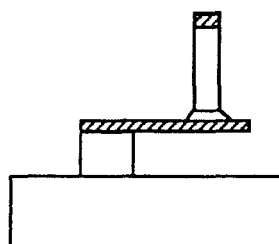
ion  
imp




D) Etch the oxide mask.



E) Form the optical switch by anisotropic etching.



Ox. p++  


**Figure 2.9** A layout of the basic fabrication steps of an optical switch using ion implantation to introduce heavily doped boron layer.

### **2.6.3. Spin On Doped Glass Approach**

This process is similar to ion implantation process mentioned in the previous section except for the introduction of the dopant in the sample. Fig. (2.10) shows the basic fabrication steps for this approach which can be summarized as

#### **A) Mirror Formation**

Review section (2.6.2) for the complete steps.

#### **B) Etch Stop Layer Formation**

- 1) Use wet oxidation to form oxide mask against the spin on glass diffusion.
- 2) Define the cantilever pattern using positive or negative photoresist.
- 3) Dope the sample using spin on glass.
- 4) Etch away the oxide mask.

#### **C) Cantilever Formation**

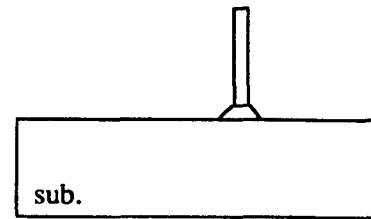
Repeat the same step in section (2.6.2).

This approach has the advantage of getting very high doping concentration levels. The control of the boron layer thickness is relatively easy using this approach. The main disadvantage for this approach is the processing difficulties experienced during photolithography. Also, there is a problem associated with protection of the mirrors' sidewalls against KOH etching. These disadvantages will be discussed in chapter (5).

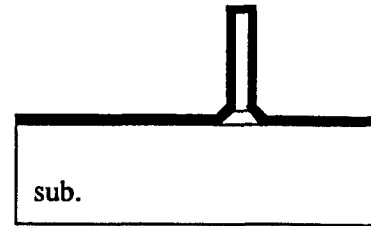
### **2.6.4. Expected Doping Profile In The Cantilever/Mirror Regions**

The resulted mirror dimensions should be  $40 \times 40 \mu\text{m}$ , and thickness in the range of  $2 \mu\text{m}$ . Due to the diffusivity factor, the boron atoms will have a certain profile within the cantilever and the mirror areas. Fig. (2.11) shows through different cross sections the predicted boron doping profile.

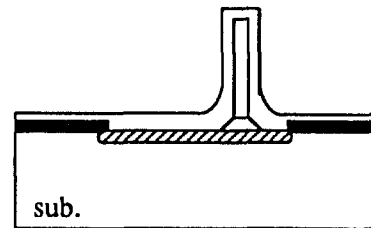
A) Form mirrors by anisotropic etching.



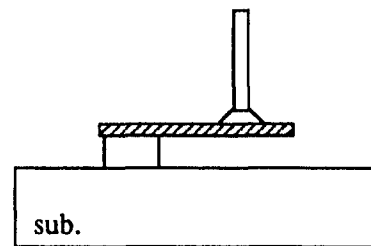
B) Form oxide mask by wet oxidation.



C) Spin on doped glass then diffuse the boron into the sample. Etch the oxide mask afterwards.



D) Form the device by KOH etching.



p++ Ox.

A legend for the diagram showing a hatched box labeled "p++" and a solid black box labeled "Ox.".

**Figure 2.10** A basic layout of processing step to fabricate an optical switch by introducing a heavily doped boron layer using spin on doped glass.

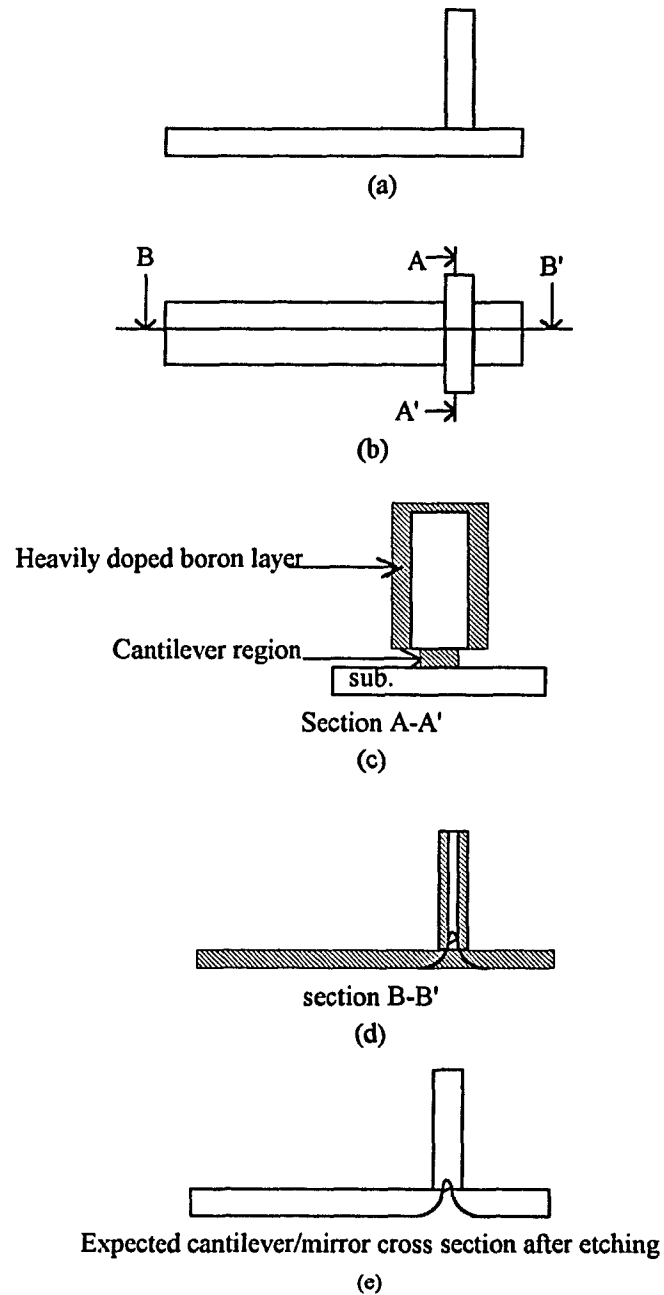


**Figure 2.11** A figure that shows the expected doping profile of boron in the cantilever/mirror regions. In (a) and (b), the sideview and the plan are shown. While the cross section A-A' shows the boron profile in the hatched area, which will depend on the boron diffusivity. Also, section B-B' shows that some of the boron atoms may not diffuse through the entire mirror thickness and the region beneath it. In (e), the cross section of the expected cantilever/mirror regions after etching is shown. Notice the thickness variations under the mirror due less doping concentration.

As one can see, the boron atoms may not diffuse all the way through the entire mirror, depending on its thickness. This might affect the area under the mirror base, in which the doping profile will may take Gaussian shape. In turn, this will cause this region to have less boron, or no boron at all, depending on the diffusion length. The etching results will depend on the doping profile shape, causing an incomplete cantilever structure, as shown in (e). This will affect the device integrity. The diffusion length can be calculated by

$$L = \sqrt{Dt} \quad (2.9)$$

where

D is the boron diffusivity.

t is the diffusion time.

The diffusion length will be vary with temperature and can be calculated.

## CHAPTER (3)

### FABRICATION PROCESSES

#### 3.1. Introduction

In chapter (2), an overview of the different processes by which one can fabricate the optical switch shown in fig.(1.1) was given. In section (2.6), the necessity of using both orientation and heavily doping etch stop phenomenon to fabricate the device were explained. In the following sections the detailed fabrication and experimental processes used in this research will be presented. One can divide the optical switch fabrication steps into two major stages :

- 1) Mirror formation ;
- 2) Cantilever formation.

#### 3.2. Mirror Formation

Three dimensional structures with deep vertical walls have been reviewed by many authors<sup>(3)</sup>, <sup>(6)</sup> & <sup>(7)</sup>. Also, in 1991 R. Cornely and R. B. Marcus<sup>(4)</sup> formed an optically smooth micromirrors, with dimensions of  $40 \times 40 \mu\text{m}$  on a  $\langle 110 \rangle$  silicon wafer. For this purpose  $\langle 110 \rangle$  surface oriented Si wafers are well suited because of two sets of planes out of the six planes of  $\langle 111 \rangle$  planes are perpendicular to  $\langle 110 \rangle$  surface<sup>(6)</sup> as shown in fig. (3.1)<sup>(4)</sup>. The relative etch resistance of  $\langle 111 \rangle$  compared to that other crystallographic surfaces, in our case  $\langle 110 \rangle$ , allow us to form vertical structures <sup>(10)</sup>, review table (2.1).

In this thesis work, which aimed at fabricating a complete optical switch as shown in fig.(1.1), it was necessary to fabricate mirror structures, reproducing some of the research results of ref. (1).

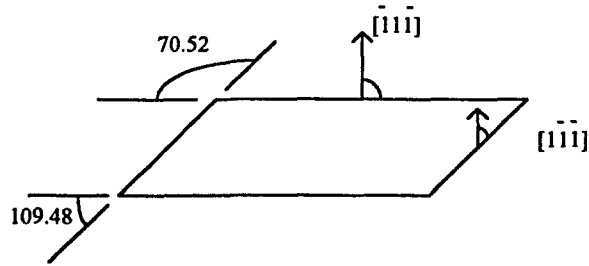


**Figure 3.1** Normal  $\langle 111 \rangle$  planes to  $\langle 110 \rangle$  planes in  $\langle 110 \rangle$  orientation silicon<sup>(4)</sup>.

### 3.2.1. General Procedure

The method used to fabricate the mirrors consisted of two stages. In the first stage, photoresist is used to define silicon dioxide pattern. In the second stage, KOH solution used to etch the mirrors. The starting Si wafers used were parallelograms with about 2" sides with thicknesses of 10-20 mils range. In all etching processes, the KOH solution was held in a Teflon container surrounded by a jacket of water heated on a hot plate at steady temperature ( $\pm 2$  °C). Magnetic stirring was used to provide agitation to keep the KOH solution uniform near the wafer and to thus obtain consistent results. Samples were held by Teflon screws against a Teflon holder that rested at the bottom of the container. The KOH solution concentration was 40% (40 gm of fresh KOH bullets : 100 ml of DI H<sub>2</sub>O). The experiments were done at 50 °C for 2-2.5 hours to form mirrors with height of 30-40  $\mu\text{m}$ .

### 3.2.2. Fabrication Steps

The following steps were done to fabricate the mirrors

#### A) Oxidation

The samples were oxidized at 1000 °C in dry oxygen for 2 hours then densified at the same temperature in N<sub>2</sub> for 15 minutes to grow 1100 to 1300 Å of SiO<sub>2</sub>.

### **B) Sample Cleaning**

Before starting the photolithography process, the sample must be cleaned so that any organic substance or contamination removed. This was done by rinsing the sample with Acetone, Methanol & Isopropyl alcohol respectively in the class 100 clean room. This procedure was used throughout this work.

### **C) Defining Alignment Regions**

By using positive photoresist AZ 1505 one can transfer a pattern of 25-200  $\mu\text{m}$  diameter circular holes which will serve to produce hexahedral shape holes bounded by  $\langle 111 \rangle$  as shown in fig. (3.2). These hexagonal shapes are used for alignment of the lines forming the mirrors with the vertical  $\langle 111 \rangle$  crystal directions in the silicon.

**The following steps of photolithography were used**

- Spin on HMDS at 600 rpm for 3 sec. for spreading.
- Spin on HMDS for 30 sec. at 4000 rpm .
- Repeat the pervious steps using AZ 1505 .
- Softbake the sample at 90<sup>o</sup> C for 30 min.
- Expose the sample for 3.5 sec. to UV at power of 15 mW/ cm<sup>2</sup>.
- Develop the sample in AZ 1:1 developer for 45 sec.
- Post bake the sample at 120<sup>o</sup> C for 30 min.

Use Buffered Oxide Etch (BOE) 6:1 to clear the circular holes from SiO<sub>2</sub> at rate of 800  $\text{\AA}/\text{min.}$ , almost 2 minutes. Then remove the photoresist using Acetone followed by the previous cleaning process.

### **D) Forming Hexahedral Shapes**

Use 40% KOH at 50  $^{\circ}\text{C}$  to etch the sample until you form a hexagonal with straight edges for easier alignment. This process should take 60 to 80 min.



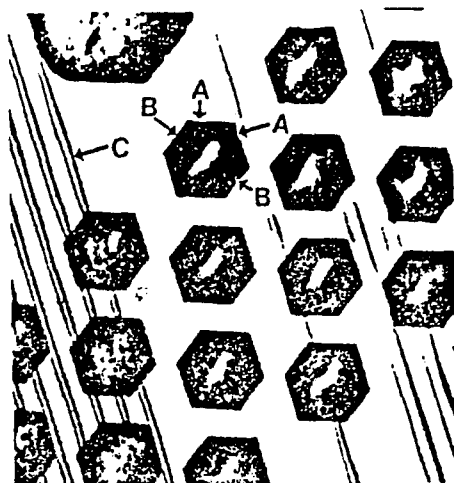


**Figure 3.2** Etched hexagonal holes in alignment region of the silicon wafer made using 50  $\mu\text{m}$  diameters circular holes in oxide mask. Marker A, B and C show the edges of the vertical and non vertical  $\langle 111 \rangle$  planes and photoresist lines, respectively. The lines were aligned parallel to the vertical  $\langle 111 \rangle$  edges and were formed using alignment region of mask 2.

Two of the three pairs of the edges of the hexagonal holes are vertical  $\langle 111 \rangle$  planes with that will serve as alignment lines for mask 2 that contain the mirror features, review fig. (3.2).

#### **E) Define Silicon Oxide Pattern For Mirrors**

Mask 2 contain alignment features consisting of 1-10  $\mu\text{m}$  opaque stripes which were aligned parallel to the correct edges of the etched hexagonal holes in the previous step. Elsewhere on mask 2 and parallel to the alignment features are 2-5  $\mu\text{m}$  wide by 132-168  $\mu\text{m}$  long opaque stripes for defining the oxide mask for the mirror. The PR AZ 1505 defined that pattern. The alignment process must be done carefully to assure a misalignment of  $0.1^\circ$ . Use BOE 6:1 to remove the oxide elsewhere on the sample except where the mirrors will be, then dissolve the photoresist as done before.

## F) Mirror Formation

Etch the sample in 40% KOH solution at 50 °C for 2-2.5 hours to form the mirrors.

### 3.3. Cantilever Formation

The second stage in fabricating an optical switch, was to form cantilever beams attached to posts for support. Mask 6 contains an opaque cantilever pattern, see fig.(3.3). Each side of the four posts' sides is aligned to  $\langle 111 \rangle$  plane. The cantilever beams dimensions varied from 20  $\mu\text{m}$  to 26  $\mu\text{m}$  wide and 100  $\mu\text{m}$  to 350  $\mu\text{m}$  long.

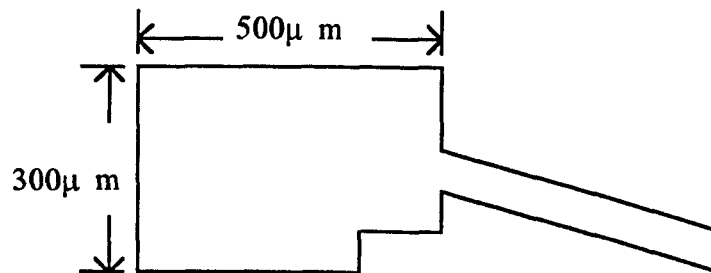


**Figure 3.3** The pattern used to form cantilever beams.

As mentioned in section (2.6), one need to introduce a heavily doped boron layer to form cantilever beams. Also, it was mentioned the possible technologies used to introduce this layer. In the following sections, the processing steps to carry out this task will be presented.

#### 3.3.1. Heavily Doped Layers Epitaxially Grown

The samples used for this experiment had 5 epi layers as mentioned in section (2.6.1). The purpose for this experiment was to study how much heavy boron doping one can get with minimum defect density to form cantilever beams with the desired thickness.

The sample used were n-type  $\langle 100 \rangle$  wafers. The sheet resistance was 6.5  $\Omega/\square$ . The total thickness of the epi layers were 34  $\mu\text{m}$  grown by SPIRE CORP. The doping

profiles of these samples were done by SOLECON LABORATORIES in California, are shown in figures (3.4), (3.5) and (3.6). To study the etching rate of the heavily doped p layers, silicon dioxide mask was deposited on part of the samples using CVD.

A similar experimental setup to the one used for mirror formation [section (3.2.1)] used as well for this experiment. A 10% KOH solution (10 gm of fresh KOH bullets : 90 ml of DI H<sub>2</sub>O) was used at 40 °C ± 2 °C.

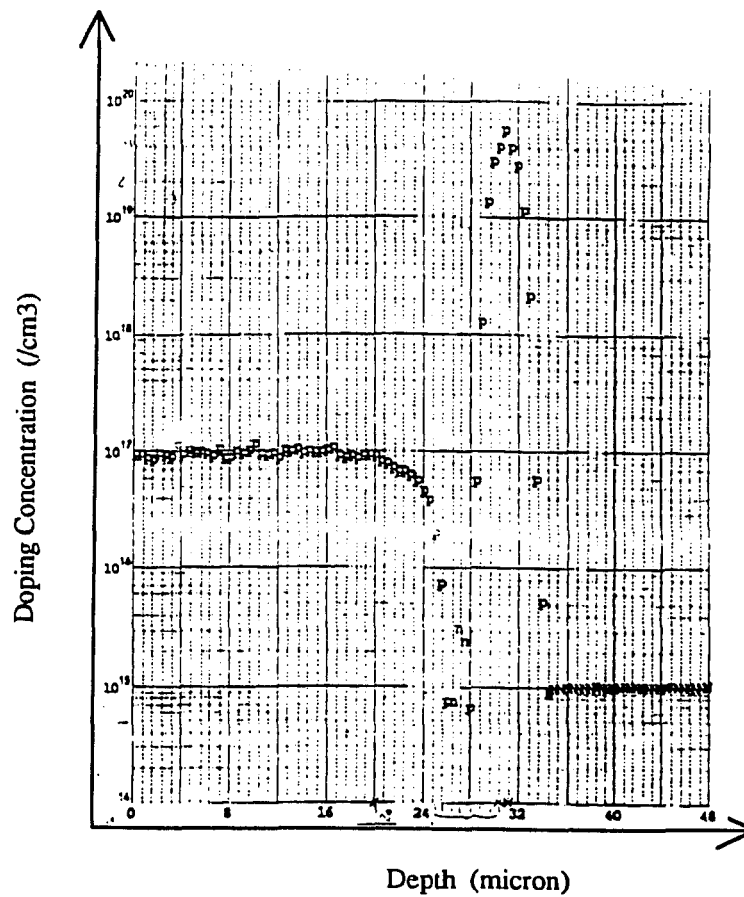


**Figure (3.4)** The doping profile of sample (1) of an epi grown layer. The maximum doping concentration was  $5 \times 10^{19} \text{ cm}^{-3}$ .

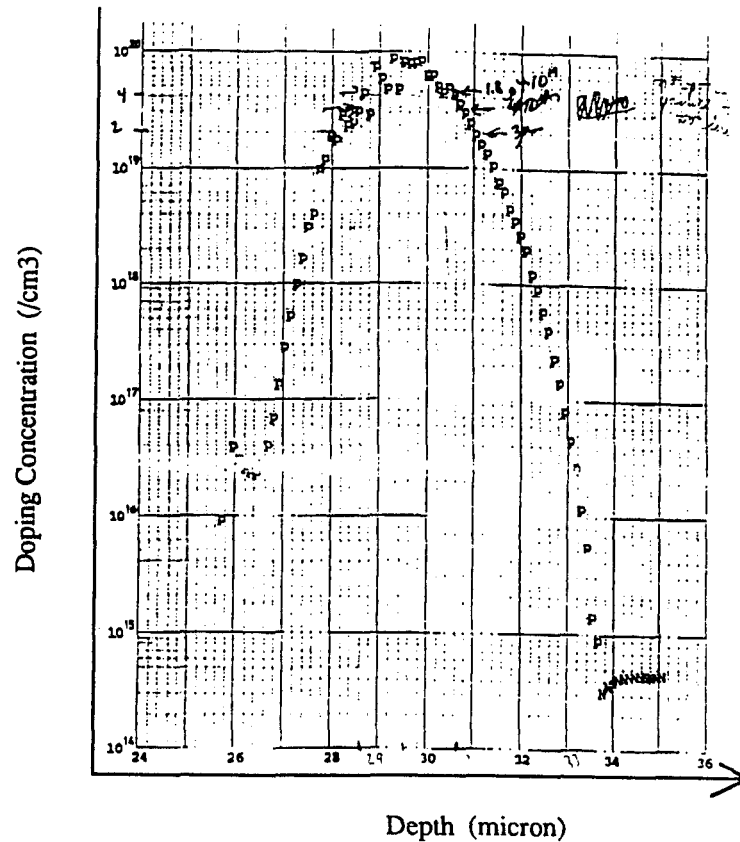


Figure (3.5) The doping profile of sample (2) of an epi grown layer. The maximum doping concentration was  $9 \times 10^{19} \text{ cm}^{-3}$ .

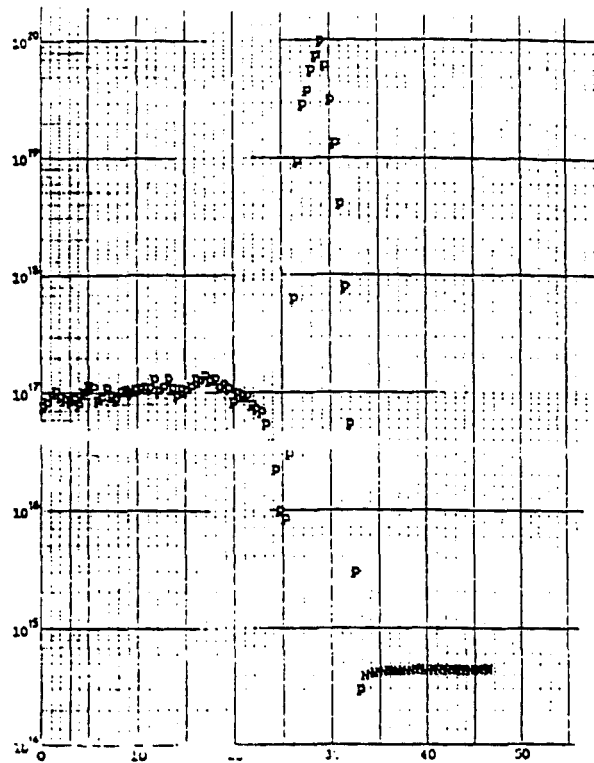


Figure (3.6) The doping profile of sample (3) of an epi grown layer. The maximum doping was  $10^{20} \text{ cm}^{-3}$ .

### 3.3.2. Heavily Doped Layers Introduced By Ion Implantation

The necessity of achieving higher boron doping concentrations so that the etch resistance of these layer can be higher lead to implement ion implantation technology to carry out this purpose.

In this experiment, an investigation to the etch rate of  $p^{++}$  was the main objective, so that the final thickness of a cantilever beam can be determined. The samples used were p and n type wafers. The process steps illustrated in fig. (3.7) can be summarized as

#### A) Oxidation

Oxidize the sample at  $1130^{\circ}\text{C}$  in  $\text{H}_2\text{O}$  environment for 7 hours, then densify at the same temperature for 15 minutes to grow  $2.2\ \mu\text{m}$  of  $\text{SiO}_2$  to mask against ion implantation.

#### B) Sample Cleaning

Repeat the same procedure mentioned in section (3.2.1.B) before the photolithography step.

#### C) Define The Cantilever Pattern

To define these regions, one can use the photoresist AZ 5214 that gives negative pattern.

**The photolithography steps were**

- Spin on HMDS at 600 rpm for 3 seconds for spreading, then spin on at 4000 rpm for 30 seconds.
- Repeat the previous steps using AZ 5214.
- Softbake at  $90^{\circ}\text{C}$  for 30 minutes.
- Expose the sample for 5.5 seconds to UV light at power of  $15\ \text{mW}/\text{cm}^2$ .
- Using hot plate at  $120^{\circ}\text{C}$  to bake the sample for 30 seconds.

A) grow 2.2  $\mu\text{m}$  oxide mask by wet oxidation for 7 hours at 1130 C.



UV  
MASK



B) Spin on PR AZ 5214, to define the cantilever regions.

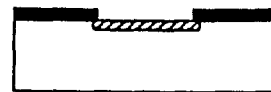
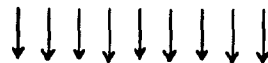


C) Etch the oxide mask except where the cantilevers pattern will be.

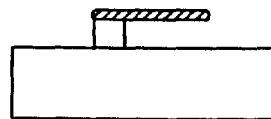


D) Use Ion Implantation to introduce p++ layer then anneal the sample at 1000 C for 30 minutes.

II



E) Using 40% KOH form a step of 40  $\mu\text{m}$  at 50 C for 2-2.5 hours.



OX PR p++

**Figure 3.7** A basic layout of a cantilever beam formation by using ion implantation to introduce heavily doped boron layer.

- Flat exposure to the sample for 9 seconds at power of  $15 \text{ mW/cm}^2$ . Notice that the accuracy of the UV power were  $\pm 0.2 \text{ mW/cm}^2$ .
- Develop the sample in AZ 1:1 for 45 seconds.
- Using the Bellcore Nanospec, check on the thickness of the photoresist for completeness of the developing.
- Postbake the sample at  $120^\circ\text{C}$  for 30 minutes.
- Check the resultant thickness of the photoresist using Nanospec.

To clear the cantilever pattern from oxide, one can use BOE 6:1 at etch rate of  $800 \text{ \AA}/\text{min}$ . 25-30 minutes are required for each sample. Notice that we have to agitate the sample to assure etching uniformity of the oxide mask.

#### **D) Ion Implantation**

In the Ion Implantation process, different dosage were used to achieve higher doping levels, i.e. 1, 1.5, 2 and 2.5 doses (see appendix A for doses). The basic (one) dose achieves  $10^{20} \text{ cm}^{-3}$  of boron concentration. According to the implantation data one should have  $0.8 \text{ \mu m}$  thick of boron layer before annealing.

#### **E) Annealing**

After ion implantation one must anneal the samples to activate the boron atoms, because of the damage and displacement of many boron atoms of the target caused by the process. The annealing temperature was  $1000^\circ\text{C}$  and was done for 15 and 30 minutes periods.

#### **F) Cantilever Beams Formation**

Use straight HF to etch the oxide mask and passivate the sample surface, then dry the sample by blowing dry  $\text{N}_2$  air to prevent it form oxidizing. To form the cantilevers, one

can use 10 % KOH solution at 50 °C for 2-2.5 hours to form 30-40 μm step according to published experimental data (10).

### **3.3.3. Heavily Doped Boron Layers Introduced By Spin On Diffusion**

To reach even a higher doping concentration one can use spin on doped glass. In this research Borosilica 100 manufactured by ALLIED SIGNAL, NJ, with doping concentration of  $5.10^{20} \text{ cm}^{-3}$ . The samples used were n-type large enough to avoid edge bads during photolithography processing. The process steps illustrated in fig (3.8) are summarized as follow

#### **A) Oxidation**

Oxidize the sample at 1050 °C in H<sub>2</sub>O environment for 1 hour then densify at the same temperature for 20 minutes in N<sub>2</sub> to grow 5000 Å of SiO<sub>2</sub> to mask the sample against the boron diffusion.

#### **B) Sample Cleaning**

Review sec. (3.2.1.B) for cleaning before photolithography.

#### **C) Defining Of The Cantilever Pattern**

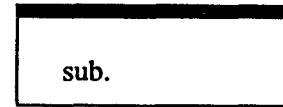
Use PR AZ 5214 to define the cantilever regions following the same steps as in section (3.3.2)

#### **D) Spin On Diffusion**

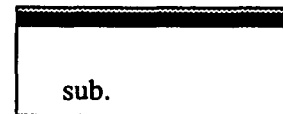
- Spin on borosilica 100 at 3000 rpm for 30 seconds.
- Cure the sample at 100 °C for 30 minutes, then at 175 °C for another 30 minutes to evaporate the solvents in the coating layer and increase the adhesion to the sample.
- Diffuse the boron into the sample at 1100 °C and in 97% N<sub>2</sub> - 3% O<sub>2</sub> for one hour.



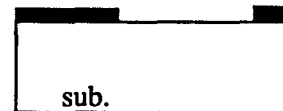
A) Grow 5000 Å of oxide mask using wet oxidation at 1050 C for 1 hour.



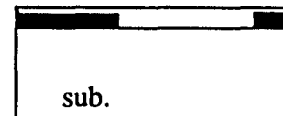
B) Spin on PR AZ 5214 to define the cantilever regions.



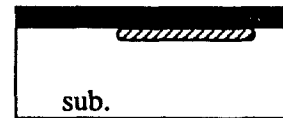
C) Etch the oxide mask except where the cantilevers are using BOE.



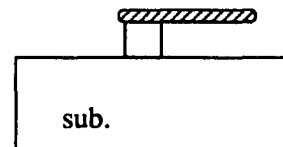
D) Spin on Borosilica at 3000 rpm for 30 seconds.



E) Cure the sample at 100 C & 175 C for 30 minutes each, then diffuse the boron at 1100 C for one hour.



F) Using 40 % KOH, form a 40 μm step at 50 C for 2-2.5 hours to form the cantilever beam.



ox. p++ sog



**Figure 3.8** A layout of a cantilever beam formation using etch stop layer introduced by spin on doped glass.

### **E) Cantilever Formation**

Repeat the same etching experiment done in ion implantation process in the previous section.

## **3.4. Fabrication Of An Optical Switch**

The aim of this research, beside studying etch resistance of heavily doped p layers, was to fabricate an optical switch as in fig. (1.1). To achieve this goal one can use the spin on doped glass technique to introduce the  $p^{++}$  layer into the sample. In this technique one has to oxidize the sample to form a mask of 5000 Å thick oxide. If the mirrors thickness is 2 μm, 44% of the total mirror thickness will be consumed in the oxidation process. This means a loss of 0.44 μm from the original thickness. Taking into considerations the etching rates of the <111> planes, or doped <111> planes, this will be a very thin mirrors for the purpose of device fabrication. A new mask 7 made to overcome this problem. The mirror thicknesses varied from 2 μm to 5 μm on the new mask. Another modification was made on the same mask, is that the posts of cantilevers pattern replaced by a bigger one to save the posts from breaking. Two different techniques were used to achieve this purpose. In the first the positive thick photoresist AZ 4620-E was used. In the second technique, the thin photoresist AZ 5214 was used.

### **3.4.1. Thin Photoresist Approach**

The fabrication process steps illustrated in fig (3.9) are summarized as follow

#### **A) Mirror Formation**

Repeat the same steps in section (3.2) to form mirrors.

**B) Sample Cleaning**

Following each etching step rinse the sample very well with DI water to stop the etching process. Dry the sample with N<sub>2</sub> air blower to prevent oxidation of the samples. Before the oxidation step, clean the samples using the standard process we used in section (3.2) to make sure that no contamination or organic substance on the surface.

**C) Oxidation**

Repeat the oxidation step done in section (3.3.3)

**D) Sample Cleaning**

Repeat the standard procedure in section (3.2).

**E) Define The Cantilever Pattern**

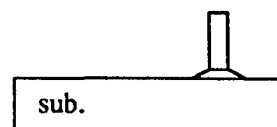
Use the standard procedure of the photolithography process mentioned in section (3.3.2), except for the alignment regions, which will be a little different as follows

Use the alignment regions of the cantilever pattern for careful alignment with the mirrors. To keep misalignment minimum, use the high magnification of optical microscope for this purpose. The soft contact mode of the mask aligner will be used, to prevent mirrors breakage. also a clearance of 3-5  $\mu\text{m}$  between the top of the mirrors and the mask must be left, see fig. (3.10). Also, the mirror should be about 5-10  $\mu\text{m}$  away from the free tip of the cantilever.

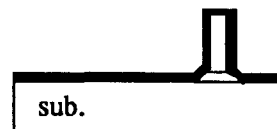
**F) Spin On Glass Diffusion**

Repeat the same process in section (3.3.3). Use straight HF to etch the oxide mask, and passivate the sample's surface to be ready for the etching process.

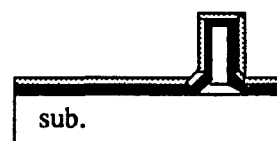
A) Form mirrors by anisotropic etching.



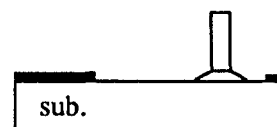
B) Using wet oxidation, form an oxide mask of 5000 Å at 1050 °C for 1 hour.



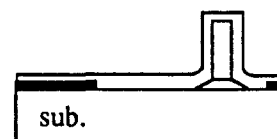
C) Spin on PR AZ 5214.



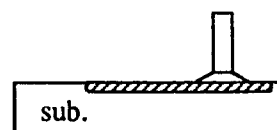
D) Print the cantilever pattern on the the sample, then etch aw the oxide mask except where the cantilevers will be. Then remove the PR.



E) Spin on Borosilica 100 (doped glass) at 3000 rpm for 30 seconds.



F) Cure the sample, then diffuse boron at 1100 °C for one hour. Etch all oxide mask using HF.



G) Using 10 % KOH solution, form the optical switch at 50 °C for 2-2.5 hours.

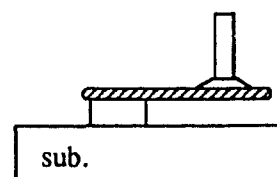
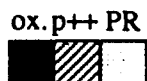


**Figure 3.9** A layout of the fabrication steps of an optical switch using thin negative photoresist AZ 5214.

### G) KOH Etching

Use 10 % KOH at 50 °C to etch the sample for 2-2.5 hours to form an optical switch.

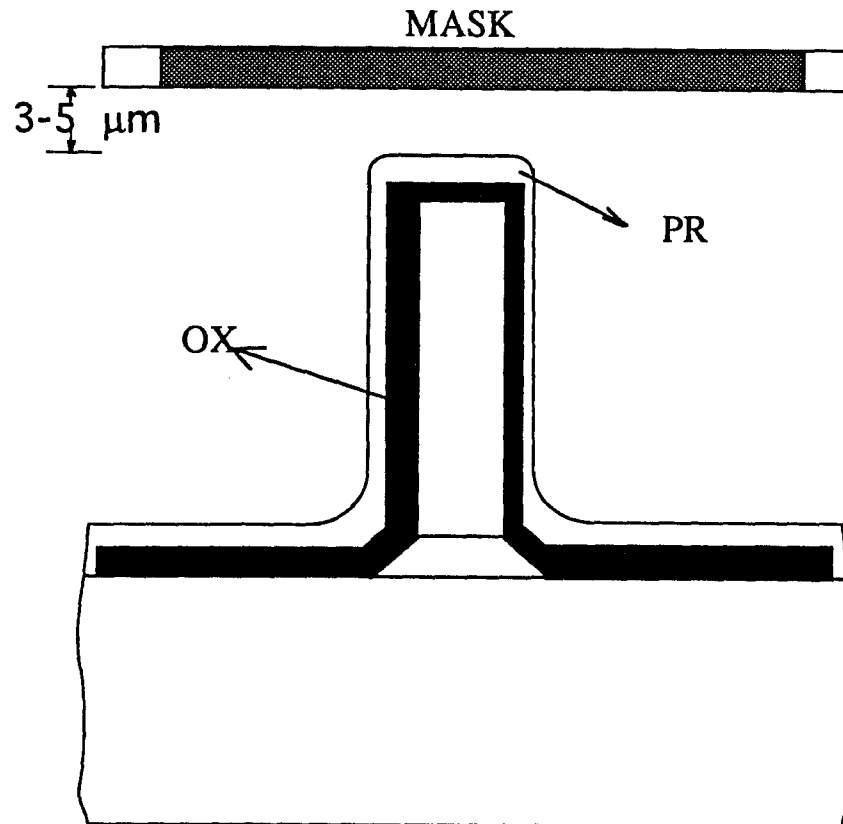


**Figure 3.10** A cross section of the mask and the sample shows their relative positions during the exposure step to transfer the cantilever pattern to the oxide mask to fabricate an optical switch.

#### 3.4.2. Thick Photoresist Technique

Using the positive photoresist AZ 4620-E one can produce thick layers of photoresist, 19  $\mu\text{m}$  for each run. The advantage of this process is to minimize the probability to break the mirrors during the alignment process, beside good contact between the mask and the sample at a good vacuum during alignment is achieved, which will improve the resolution.

Fig. (3.11) shows the process steps for this technique which can be summarize as follow

**Repeat the steps from A to E as in section (3.4.1).**

## **F) Defining The Cantilever Regions**

**The following photolithography steps were done to define the cantilever pattern using mask 7**

- Clean the sample using the standard procedure in section (3.2)
- Spin on HMDS at 930 rpm for 30 seconds.
- Spin on PR AZ4620-E at 930 rpm for 30 seconds.
- Soft bake the sample at 90 °C for 5 minutes.
- Spin on AZ 4620-E at 930 rpm for 30 seconds.
- Softbake the sample at 90 °C for 1 minute.
- Use Q tips wet with acetone to carefully remove the edge bads.
- Softbake the sample at 90 °C for 60-70 minutes. Let the sample to cool down for 20 minutes before starting the alignment and exposure process. This will allow the sample to absorb more moisture which will improve the exposure results.
- Align the sample similar to what was done in section (3.4.1) using hard contact mode of the mask aligner, see fig. (3.12)
- Expose the sample to UV light for 2.25 minutes at  $(15 \pm 0.2) \text{ mW/cm}^2$ .
- Develop the sample in straight AZ 421 for 3.5 minutes.
- Use hot plate at 120 °C to postbake the sample for 30 seconds. You might skip this step.

Use BOE or Reactive Ion Etching to clear the oxide mask off the sample except where the cantilevers are. Then remove the photoresist using Acetone, Methanol and Isopropyl respectively.

At 1100 °C diffuse the boron in N<sub>2</sub> for 1 hour. Clear the oxide mask using straight HF and the sample will be ready for KOH etching.

A) Form mirrors .

B) Form oxide mask of 5000 A thickness by wet oxidation at 1030 C for 1 hour


C) Spin on doped glass, then cure the sample at 100 C & 175 C for 30 minutes each.

D) Spin on PR AZ 4620-E .

E) Print the cantilever pattern on the sample, then using RIE, etch the borosilica off all the sample except where the cantilever beams will be. Then remove the PR.

F) Diffuse the boron at 1100 C for one hour. Etch the oxide using HF.

G) Using 10 % KOH solution, form the cantilever beam system at 50 C for 2-2.5 hours.

ox. p++  

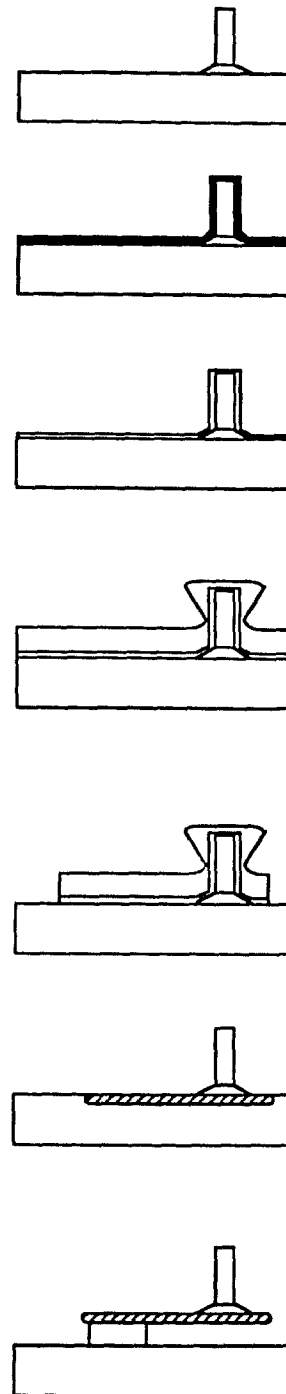



**Figure 3.11** A layout of the fabrication steps of an optical switch using thick positive photoresist AZ 4620-E.

**G) KOH Etching**

Etch the sample in 10 % KOH at 50 °C for 2-2.5 hours as in section (3.4.1).

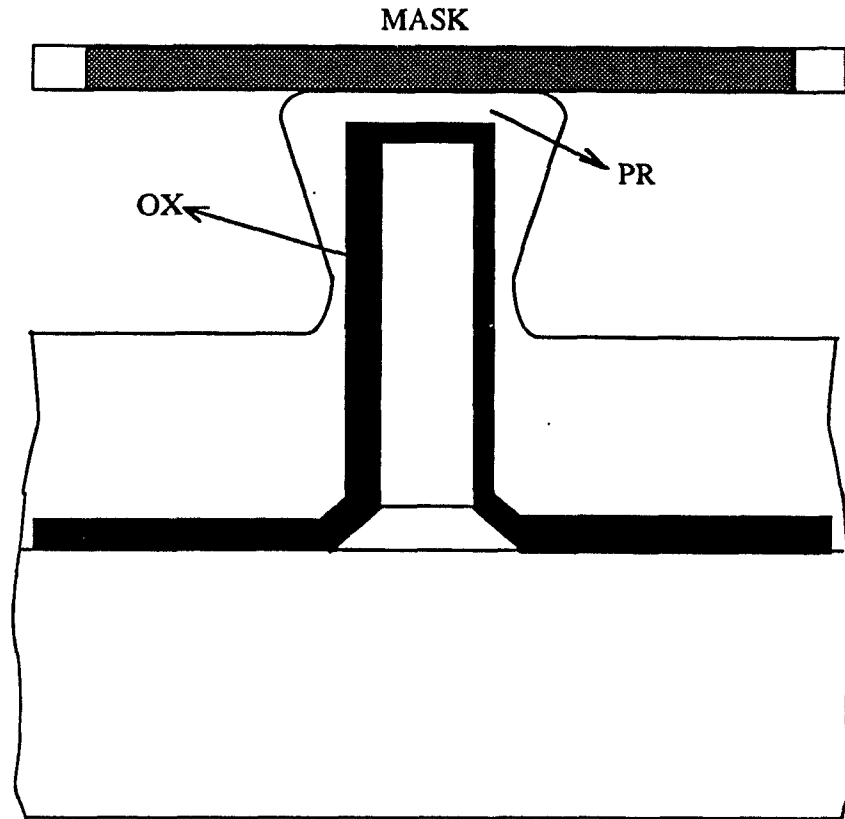


**Fig. 3.12** A cross section shows the relative positions of the mask and the sample during the exposure step to transfer the cantilever pattern to the oxide mask using thin negative AZ PR 5214.



## **CHAPTER (4)**

### **EXPERIMENTAL RESULTS**

#### **4.1. Introduction**

In chapter (3), an overview of the processing steps were introduced. These experiments were used to determine how slowly the heavily doped boron layers will etch. This will give an idea of how heavy doping one can get with good quality  $p^{++}$  layers. Different technologies were used to achieve this goal as mentioned before.

The experimental results can be divided according to the subject of interest to:

- 1) Study of the etch resistance of heavily doped boron layers;
- 2) Study of the surface roughness of the wafer surface due to KOH etching;
- 3) Study of the reliability of fabricating an optical switch by using spin on doped glass (SOG) to introduce the etch stop layers.

In the following sections, the experimental results will be introduced in a sequence depends on the technologies used to introduce the  $p^{++}$  layers.

#### **4.2. Mirror Fabrication Results**

In fig. (4.1.a) and (4.1.b), the SEM micrographs of the mirror fabrication result are shown. The resultant thickness of the mirror was 1.6  $\mu\text{m}$ , fig. (4.1.a), while the mirror height was 25  $\mu\text{m}$ . This was the result of 2 hours etching in 40% KOH followed by 5 minutes of etching in 40% KOH plus 25% isopropyl solution.

#### **4.3. Epitaxially Grown Layers results**

##### **4.3.1. Surface morphology results**

A drawing of the sample surface morphology as observed using optical microscope

is shown in fig (4.2). This sample was etched for one hour in 10% KOH at 40 °C. One can see a scattered pattern of gray and white regions. The white regions were smooth and highly reflective with high etch resistance. These regions believed to be heavily p doped. While the gray regions were not smooth and scattered the microscope light. These regions are believed to be non uniformly doped or with high concentration of point defects. The etching rate measurements will be presented in the following section.

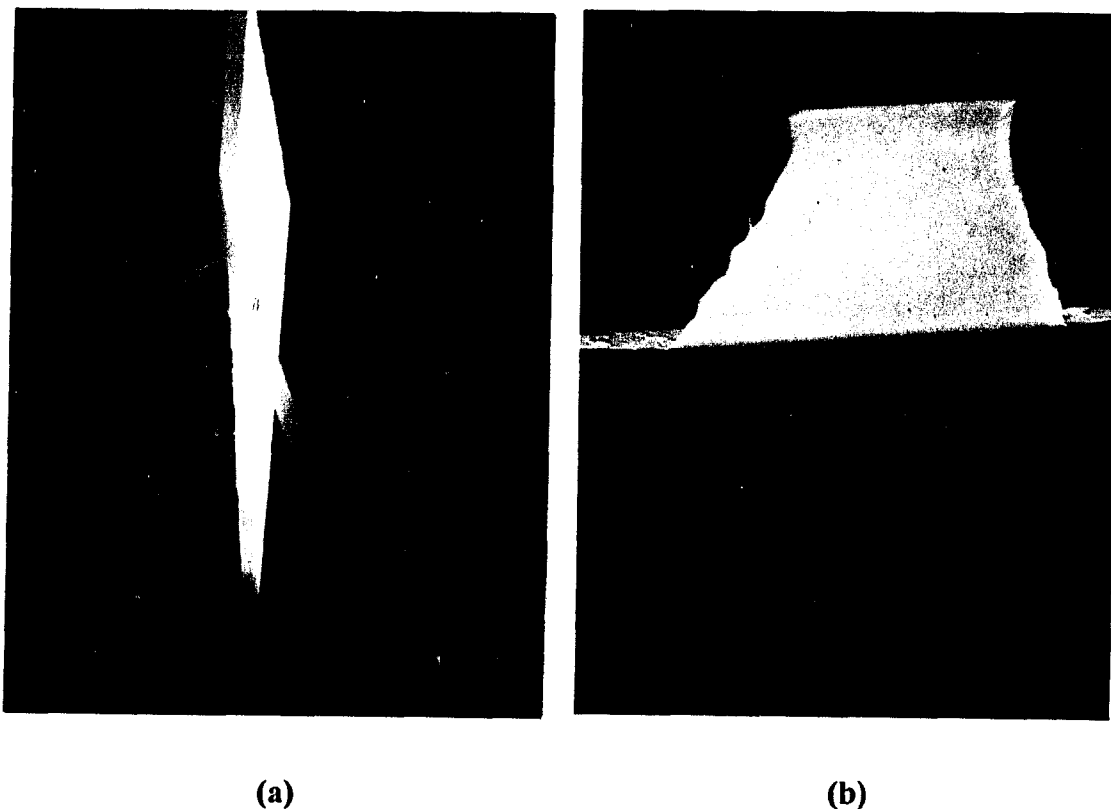


**Figure 4.1** SEM micrograph for an etched mirror in 40% KOH solution for 2 hours followed by 5 minutes of etching in (40% KOH + 25% Isopropyl alcohol) solution at 50 °C. a) A sideview, and b) a front view of the mirror.

shown in fig. (4.2). This sample was etched for one hour in 10% KOH at 40 °C. One can see a scattered pattern of gray and white regions. The white regions were smooth

and highly reflective with high etch resistance. These regions believed to be heavily p doped. While the gray regions were not smooth and scattered the microscope light. These regions are believed to be non uniformly doped or with high concentration of point defects. The etching rate measurements will be presented in the following section.

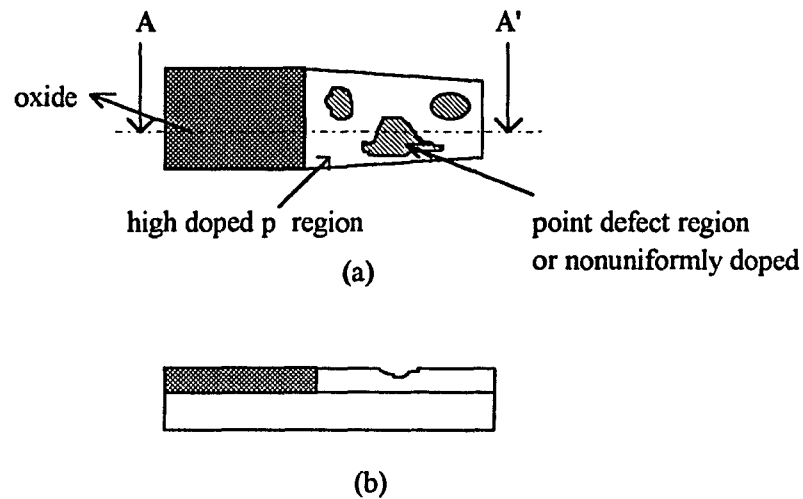


**Figure 4.2** A top view (a) and side view (b) of an etched epi grown layer of heavily doped boron relative to an oxide mask. It is clear the cause of the different etch rates of the white (heavy doped p) and the gray (high density point defects) regions.

#### 4.3.2. Etching Rate Results

The etching curves of samples whose doping profiles were given in chapter (3) are shown in fig. (4.3) to fig. (4.5), respectively. Notice that the etching rates (curves' slopes) were relatively similar for both regions gray and white in first 20  $\mu\text{m}$  of the epi layer thickness.

Also, the etching rate slowed down after this regions for the white regions, specifically in 20  $\mu\text{m}$  to 30  $\mu\text{m}$  region. The etching rate for the white region increases gradually after 29  $\mu\text{m}$ , notice the change in the curves' slopes.. On the other hand, the etching rate for the gray region hold almost steady without significant change.

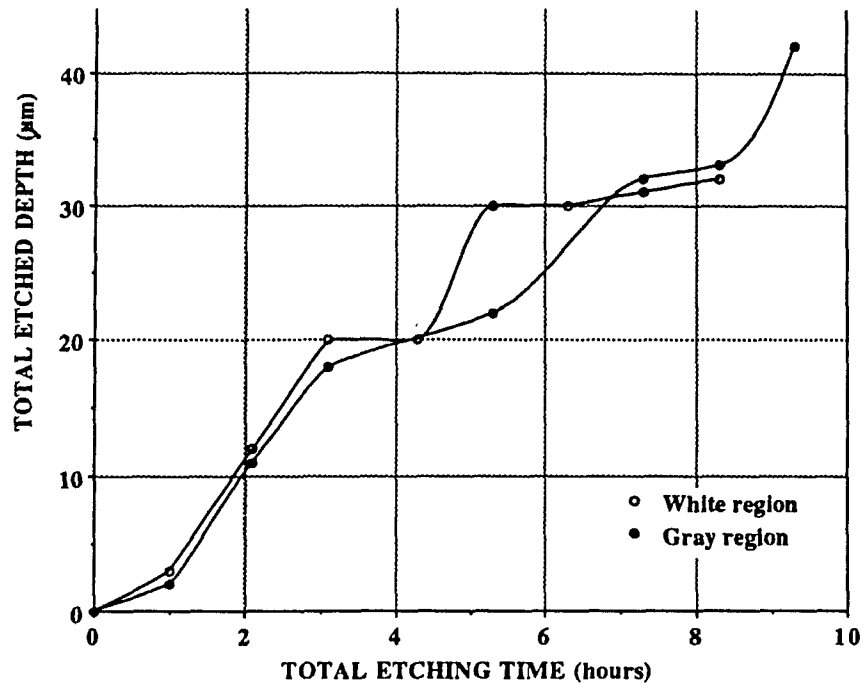


Figure 4.3 The etched depth versus time for the sample of doping profile shown in fig (3.4).

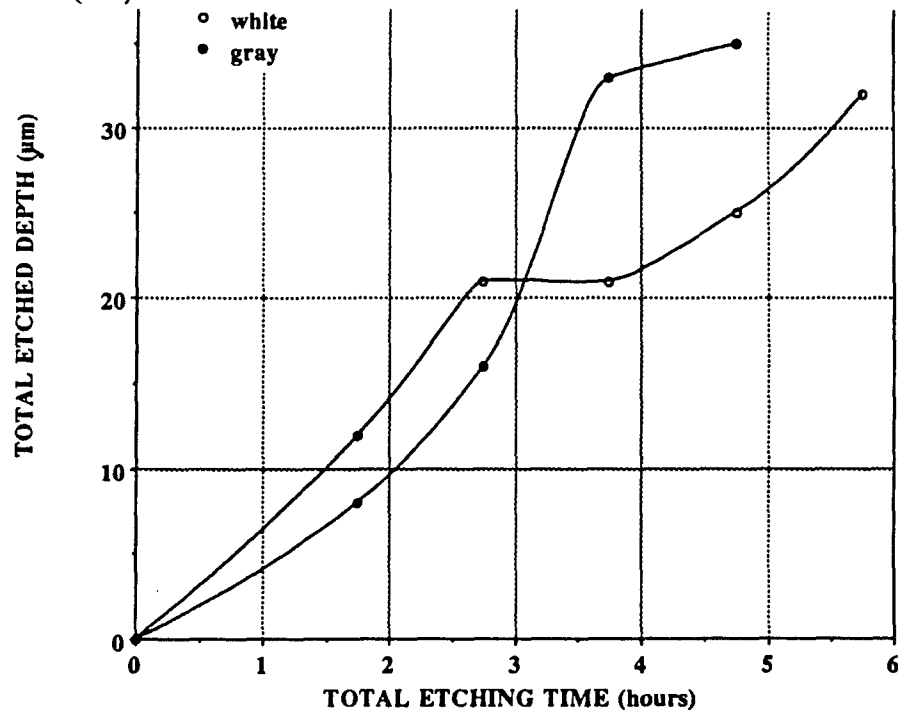
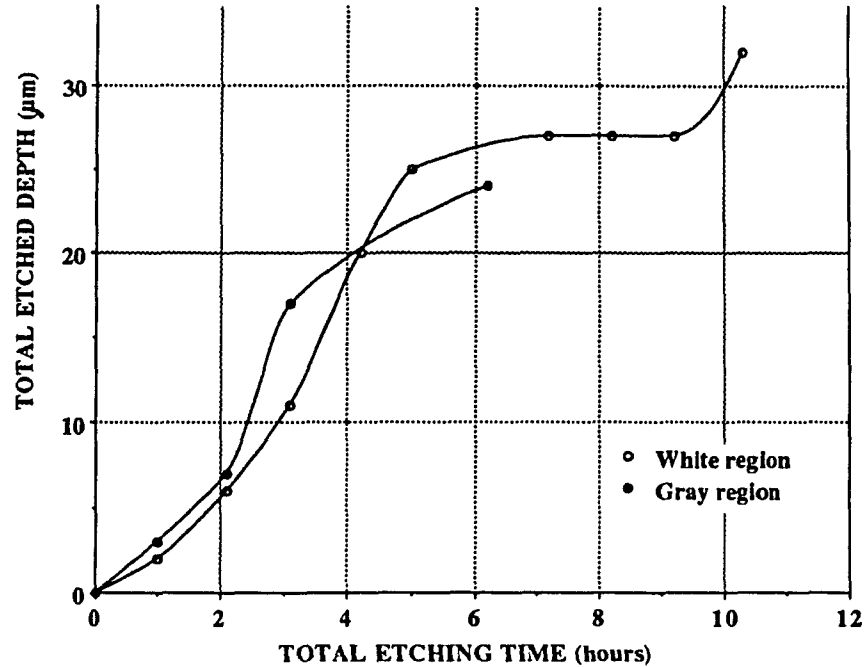


Figure 4.4 The etched depth versus time for the sample of doping profile shown in fig (3.5).



**Figure 4.5** The etched depth versus time for the sample of doping profile shown in fig (3.6).

#### 4.4. Results Of Heavily Doped Boron Layers Introduced By Ion Implantation

In the previous section, the etching results of the  $p^{++}$  layers grown epitaxially were presented. The need for higher doping concentrations and the preliminary poor results, directed the research to implement another technologies to the introduce the heavily doped layers. One of these technologies implemented was ion implantation.

In the following sections the experimental results of these experiments will be introduced. Two major points were taken into account for these results:

- Masking against Ion implantation in which three type of masks were used. The first type was PR AZ 5209 plus silicon dioxide of total thickness 3.1  $\mu\text{m}$ . The second was silicon dioxide mask only of thickness 2.2  $\mu\text{m}$ . The last was PR AZ 5214 mask only of thickness 1.4  $\mu\text{m}$ ;

- Ion implanted doses, in which a different dosages were used. 1, 1.5, 2, 2.5 doses of ions were implanted. Appendix A shows a single dose of implanted ions which gives maximum doping concentration of  $10^{20} \text{ cm}^{-3}$ . This dose will result in 0.8  $\mu\text{m}$  thick boron layer before annealing. The thickness calculated to be 0.83  $\mu\text{m}$  after 15 minutes annealing and 0.842  $\mu\text{m}$  after 30 minutes. The annealing temperature was 1000  $^{\circ}\text{C}$ .

The results will be divided into two parts

- 1)  $\text{P}^{++}$  layer thinning and surface morphology.
- 2) The inward etching of the silicon material beneath the posts' regions versus the  $\langle 110 \rangle$  vertical etching (downward).

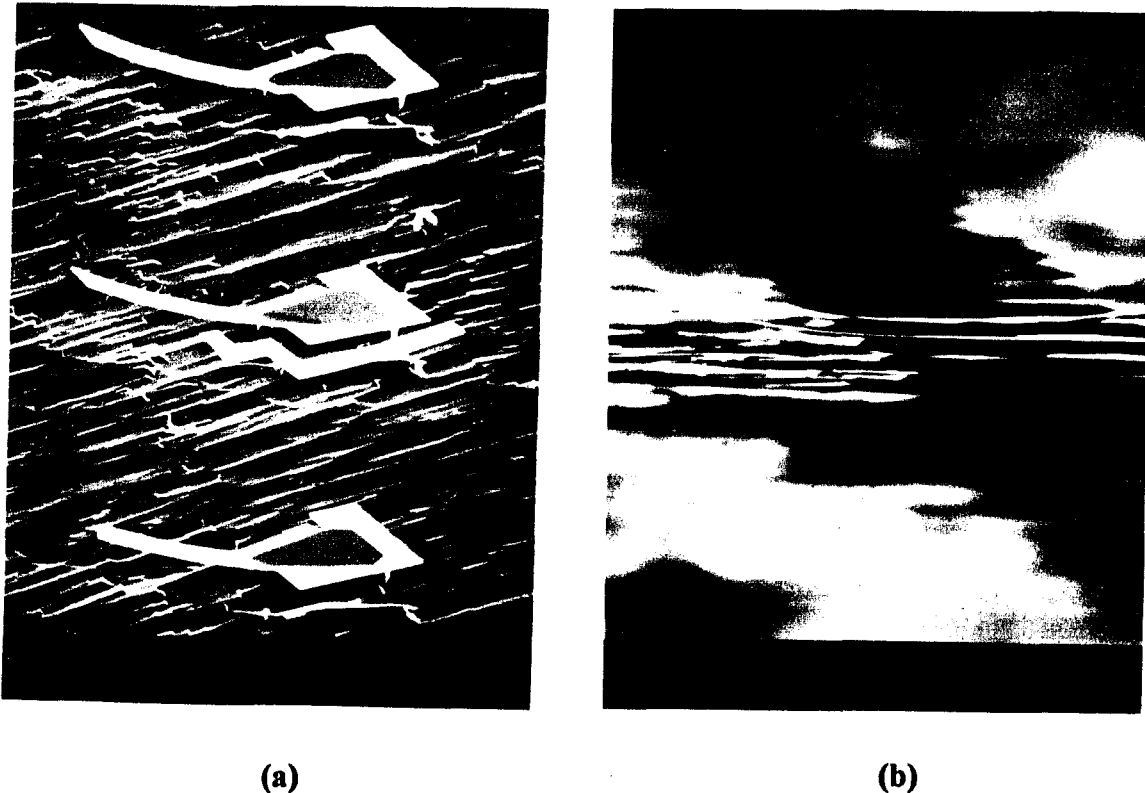
#### 4.4.1. Heavily Doped P Layer Thinning And Surface Morphology

Fig. (4.6) shows the SEM micrographs of an etched sample received 2 doses of implantation, i.e.  $2 \times 10^{20} \text{ cm}^{-3}$ . The annealing time for this sample was 15 minutes, i.e. boron layer should be 0.83  $\mu\text{m}$ . First etching trials ( 10% KOH at 50  $^{\circ}\text{C}$ ) showed that the reaction products (bubbles, as indication of etching process) were very low for 5.5 hours, then an increase in the reaction products indicated an etching rate increase occurred after 5.5 hours of etching. In the SEM micrographs, one can see:

- 1) In (a), the posts is shown to be broken from the side which is closer to the acute angle of the cantilever beams. Also, the cantilever beams are curling up by 17.5  $\mu\text{m}$  as shown in (b). This observation was for all cantilever beams longer than 150  $\mu\text{m}$ . The exception was for the short length cantilevers, 100  $\mu\text{m}$ , which were mostly straight, about 90% of the pattern;
- 2) In (c), a side view of the cantilever beam at high magnification is shown. The thickness measured was 0.44  $\mu\text{m}$ ;
- 3) Another observation is shown in (d) which is a 100  $\mu\text{m}$  cantilever beam is sticking to the sample surface. Also, notice the etched plane edges shown in black. In (e), a

trace of these planes was made and found the acute angle was  $\approx 69^\circ$ . These angles didn't change by further etching.

The second group of samples were annealed for 30 minutes. The etching curves and the optical micrographs for these samples are shown in figures (4.7) to (4.14).



**Fig. 4.6.a,b** A SEM micrographs show the etching results of cantilever beams introduced by ion implantation. This sample etched in 10% KOH at  $50^\circ\text{C}$ . In **a**), a row of cantilever beams is shown. Notice the broken cantilever side in the side of the cantilever acute angle. In **b**), a  $17.5\ \mu\text{m}$  curl up in  $350\ \mu\text{m}$  cantilever beam is shown.

The observations and results can be summarized as follows:

- 1) In figure (4.7), the optical micrograph of a sample received 1.5 doses of implantation is shown. This sample was n-type with (PR AZ 5209 + oxide) mask. Notice

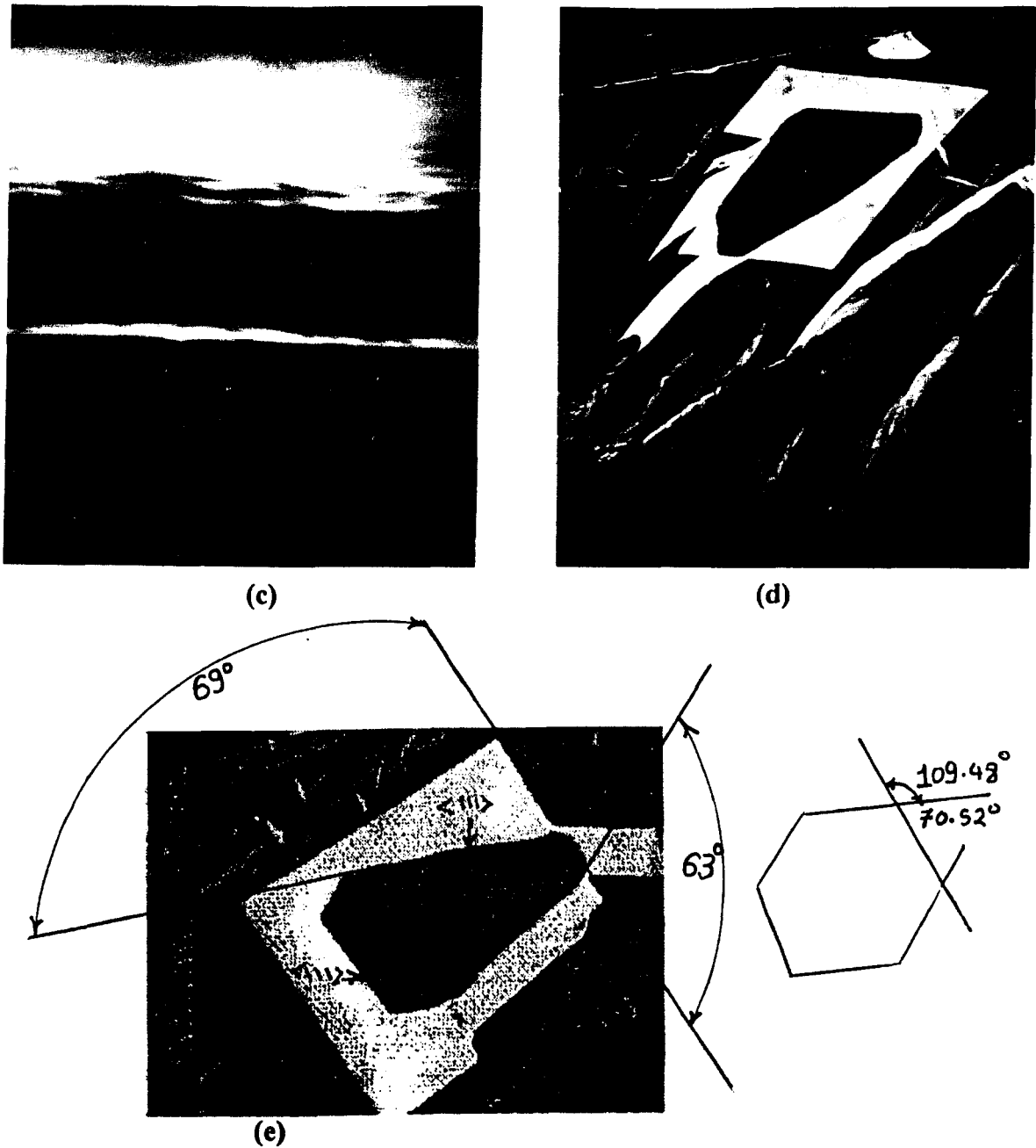


**Figure 4.6.c,d,e** In c), a  $0.44\ \mu\text{m}$  thick cantilever beam after 2 hours etching is shown. In d), a micrograph shows a  $100\ \mu\text{m}$  cantilever beam sticking to the sample surface while the close up shows clearly the broken side of the post. In e), a trace of the etched cantilever pattern shows the angles of etched planes. Notice the insert of a hexahedral etched hole<sup>(6)</sup> in  $\langle 110 \rangle$  wafer for comparison.



the black dots shown in (a) on the entire cantilever beam and the post regions. A high magnification photo in (b) shows one of these black dots pointed at by marker B. Also in (b), the etched silicon planes are pointed at by marker A. Another marker C to the trace of etched plane in the post region after 1.6 hour of etching. Also in (c), the edge of the post has a thin texture, so that you can see through the p layer. The pattern edges were jagged;

- 2) The etching rate for this sample was  $(16 \pm 1) \mu\text{m/hr}$  as shown in fig. (4.8);
  - 3) Fig. (4.9) shows the optical micrograph of another sample received 2.5 doses of implantation and had a similar mask to the previous sample is shown. The optical micrograph shows a straight sharp edges. Also a straight  $100 \mu\text{m}$  cantilever beam is shown. All other longer cantilever beams were curling up between  $10 \mu\text{m}$  and  $18 \mu\text{m}$ ;
  - 4) The etching rate for this sample as shown in fig. (4.10) was  $(14 \pm 1) \mu\text{m/hr}$ ;
  - 5) In Fig. (4.11), the optical micrographs of another sample received 2.5 doses of implantation is shown. This sample was n-type that had silicon oxide mask only of thickness of  $2.2 \mu\text{m}$ . From the photos, one can see the etched planes which pointed at by marker A in (a). Also, a firm texture and very sharp edges of the boron layer can be observed in all photos;
  - 8) The etching rate for this sample was  $(19.4 \pm 1) \mu\text{m/hr}$  as shown in figure (4.12);
  - 9) The results of the fourth sample were shown in figures (4.13) and (4.14). This sample received 2.5 doses of ion implantation and had PR AZ 5214 mask only of thickness of  $1.4 \mu\text{m}$ . The sample was p-type wafer. The optical photographs in fig. (4.13) show the sharp edges of the pattern. It can be seen the marker A in (a) pointing at the etched planes. Also, in (b) and (c) the cantilever beam were twisted in a spiral shape. About 10% of the pattern had this problem. The rest of the cantilever pattern were curling up
- The etching rate can be determined from fig. (4.14), which was  $(15.3 \pm 1) \mu\text{m/hr}$ .

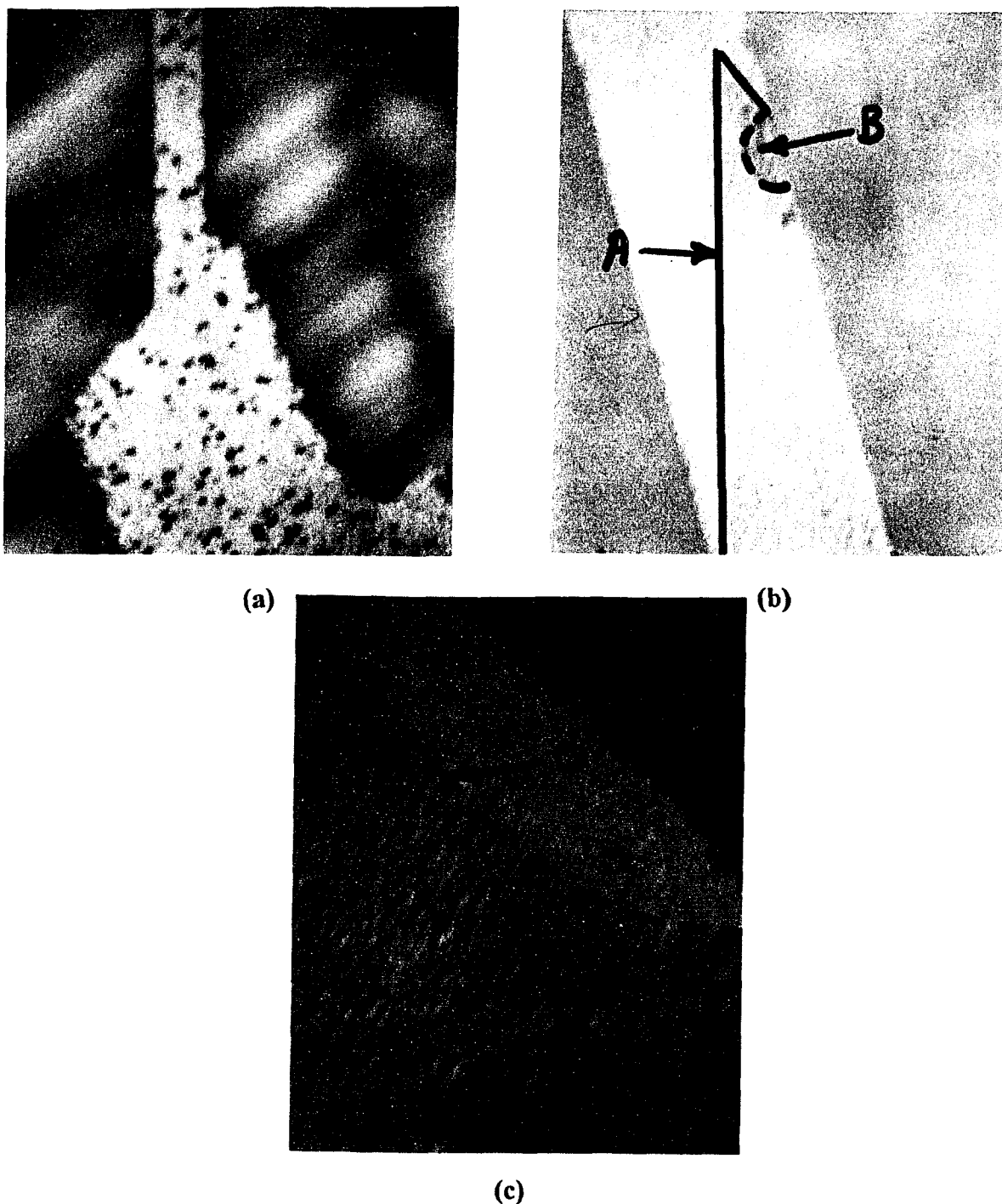


**Figure 4.7** The optical micrographs of a sample received 1.5 doses of ion implantation. Notice the thin texture of the boron layer and the jagged edges of the pattern. Also, notice the black dots scattered on the pattern (a). The high magnification in (b) shows a black dot as a valley, marker B, while marker A is pointing at etched plane in the first stages of etching. Also, marker C is pointing at the corner (inward) etching in the post's region (c).

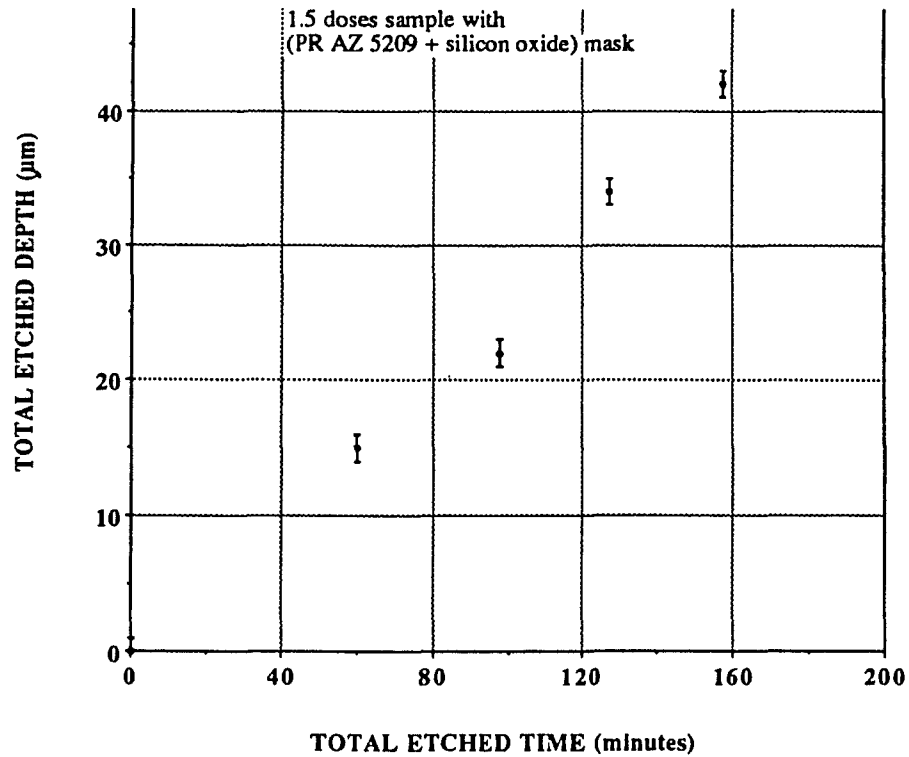


**Figure 4.8** The etching curve of the previous sample in fig.(4.7).



**Figure 4.9** The optical micrograph of a sample received 2.5 doses of ion implantation shows sharp edges and firm texture for the cantilever beam pattern. Notice the straight 100 µm long cantilever beam.

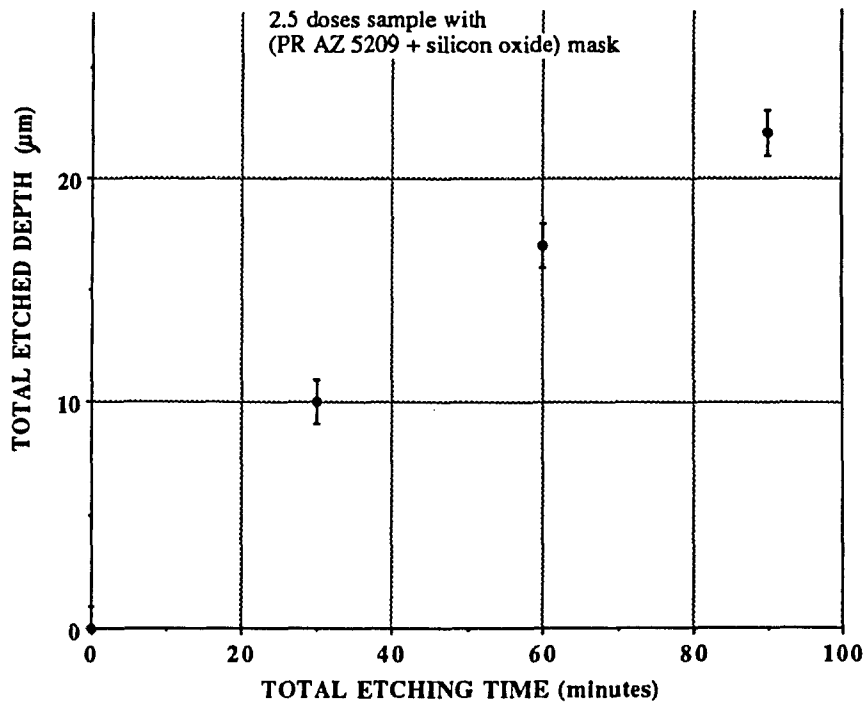


Figure 4.10 The etching curve for the pervious sample, fig. (4.9).

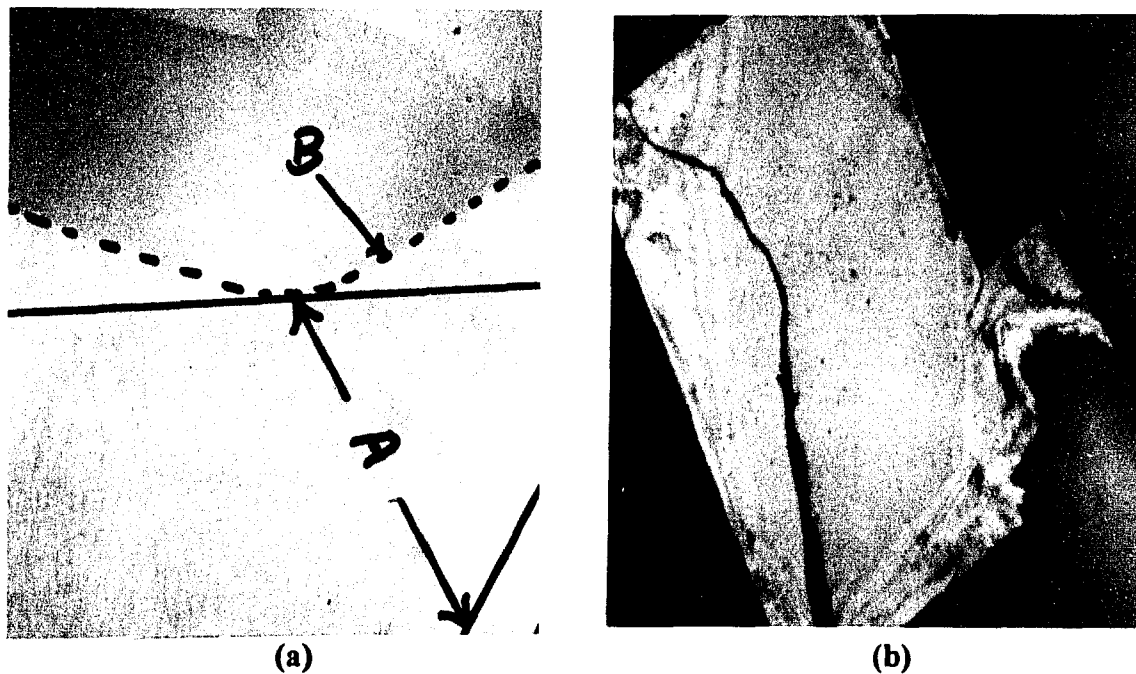


Figure 4.11 The optical micrograph of the sample received 2.5 doses of ion implantation. Notice the firm texture of the boron layer and the markers A and B are pointing at the etched planes and the post edge respectively (a). While, an etched part of the post is shown in (b). Also the crack in the boron layer was shown in about 5% of the pattern

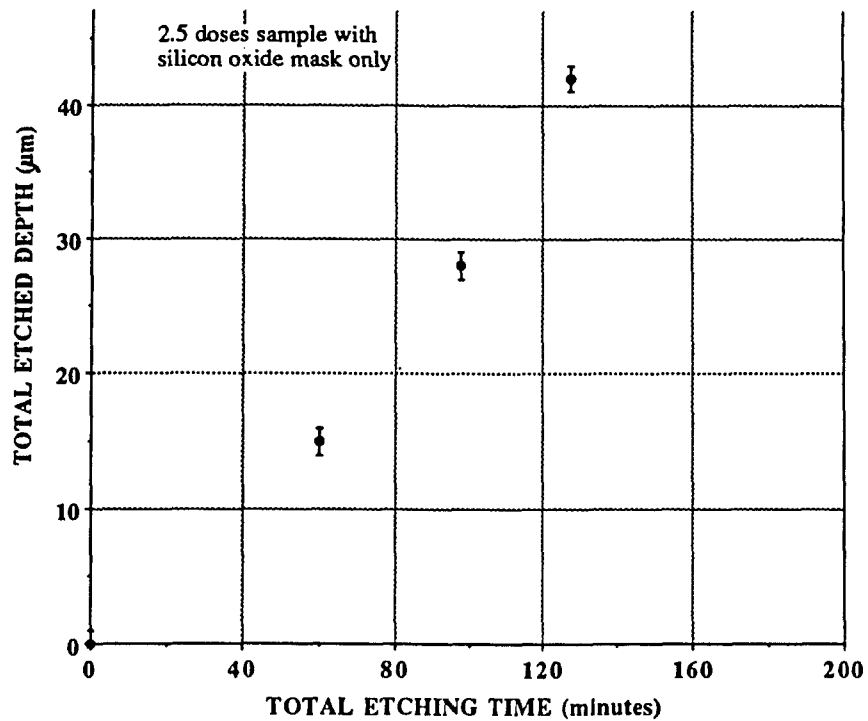


Figure 4.12 The etching curve for the previous sample, in fig. (4.11).

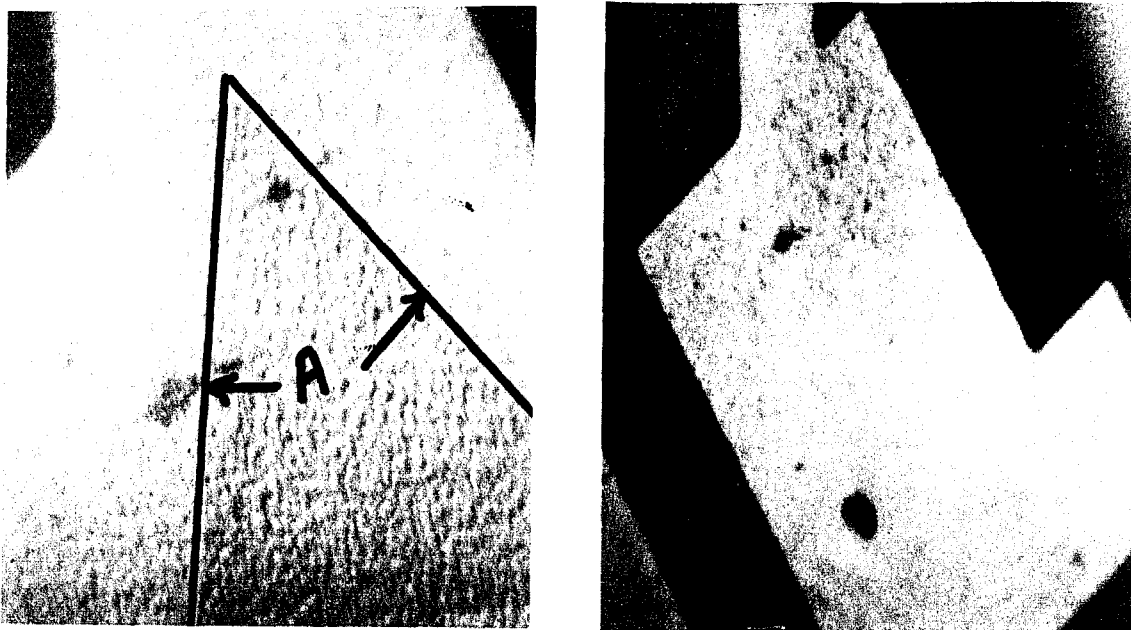


Figure 4.13 The optical micro graph for a sample received 2.5 doses of implantation. It had PR AZ 5214 mask only. Notice the marker A for the etched planes in. Also, in this sample the cantilever beams were twisted in a spiral shape.

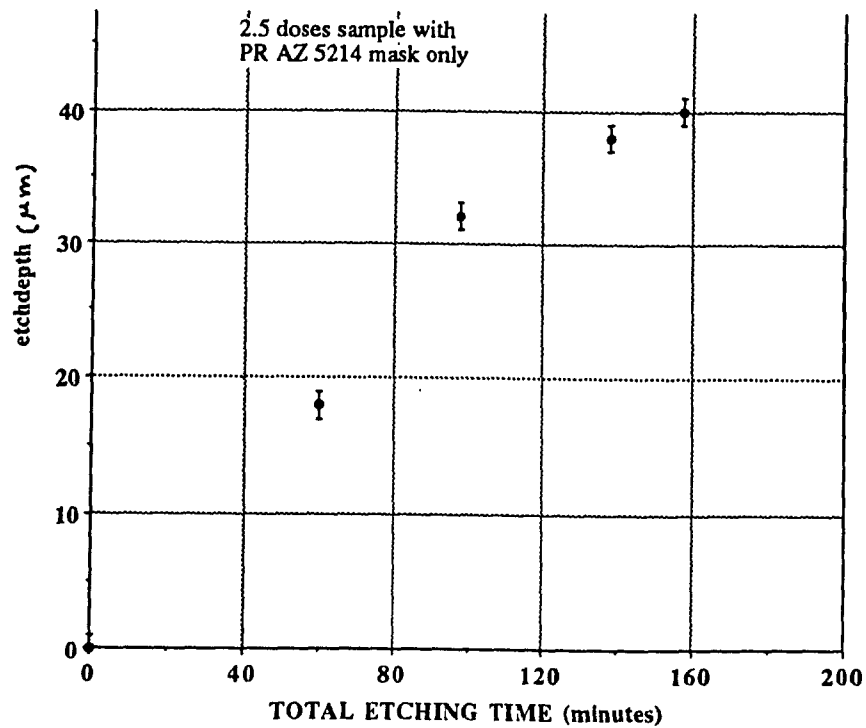


Figure 4.14 The etching curve for the previous sample fig. (4.13).

#### 4.4.2. Inward Etching Versus Downward Etching

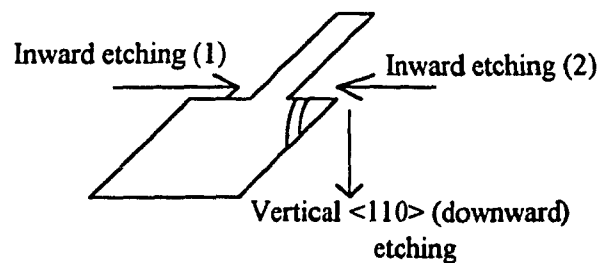


Figure 4.15 A trace of the measured inward versus downward  $\langle 110 \rangle$  etching rates.

During the experimental work, a repeated damage to the post regions from the acute angle sides was observed, see fig. (4.6.d). This suggests the lack support to these regions. A set of data were measured to relate the inward etch rate of the silicon to the

downward  $\langle 110 \rangle$  etch rate to determine how fast the silicon material beneath the post region is etching as shown in fig. (4.15).

The results are summarized in figures (4.16) and (4.17). In Fig. (4.16), the etching rate from the acute angle side (1) was  $6.6 \mu\text{m/hr}$ , while the downward etching rate was  $12.4 \mu\text{m/hr}$ . On the other hand, the etching rate from the obtuse angle side to the downward etch rate was  $14.4 \mu\text{m/hr}$  versus  $16.5 \mu\text{m/hr}$ , which is shown in fig. (4.17).

#### 4.5. Results Of Heavily Doped Layers Introduced By Spin On Doped Glass

In this set of experiments, the spin on doped glass technique was used to introduce the heavy doped layer. A doping concentration of  $5 \times 10^{20} \text{cm}^{-3}$  was achieved using this technology.

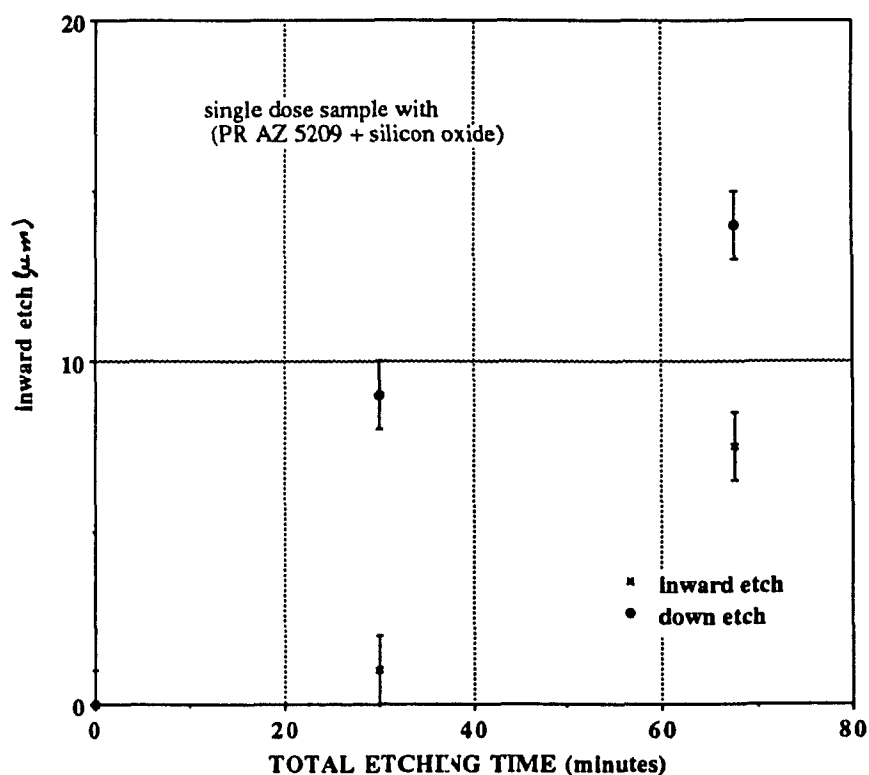
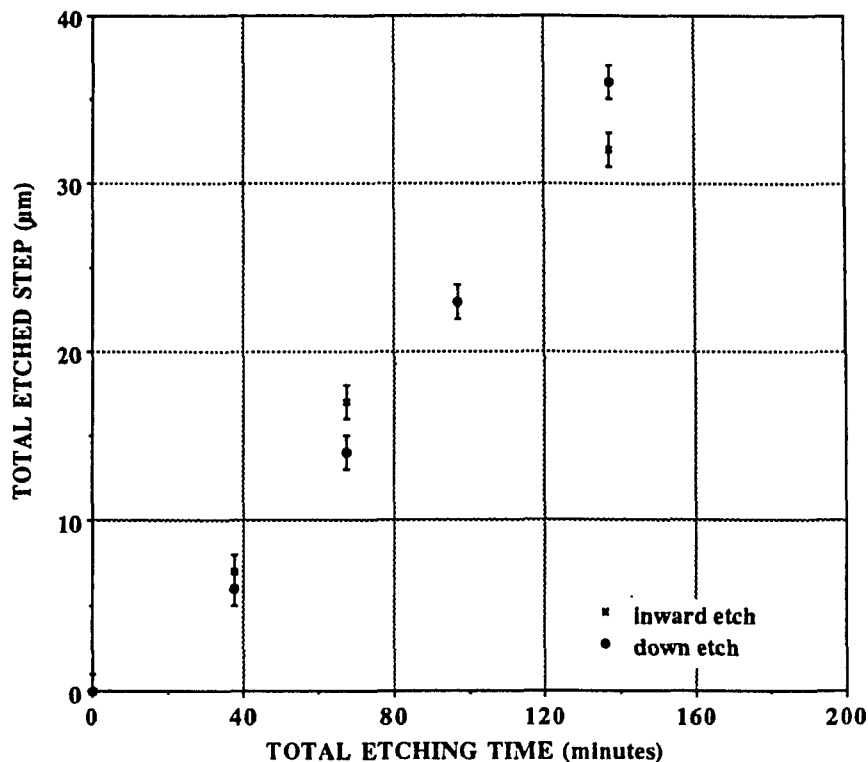


Figure 4.16 The etching results of the inward etching of the post's acute angle side versus downward  $\langle 110 \rangle$  etching.



**Figure 4.17** The etching results of the inward (obtuse angle side of the post) versus downward  $\langle 110 \rangle$  etching rates.

In the following sections the experimental results of fabricating cantilever beams will be presented

#### 4.5.1. Heavily Doped Layer Measurements

The sheet resistance technique was used to measure the heavily doped boron layer thickness. The junction depths were measured for two different diffusion temperatures.

The results were:

- 1) For a diffusion temperature of  $1100^{\circ}\text{C}$  and environment of 97%  $\text{N}_2$  - 3%  $\text{O}_2$ , the diffusion time was 60 minutes. The resultant sheet resistance was  $6 \Omega/\square$ , and thus  $X_j = 1.9 \mu\text{m}$ ;



- 2) For a diffusion temperature of 1050 °C and environment of 97% N<sub>2</sub> - 3% O<sub>2</sub>, the diffusion time was 60 minutes. The resultant sheet resistance was 13 Ω/□, and thus X<sub>j</sub> = 1.1 μm.

The first parameters in (1) were used through the rest of the spin on glass experiments, which will maximize the thickness of the boron layers.

#### **4.5.2. Cantilever Beam Fabrication Results**

The results of a cantilever beam fabrication are shown in Figs. (4.18) and (4.19). In fig. (4.18,a), the optical micrograph shows a sample etched for 30 minutes (a). One can observe the two regions indicated by white and gray colors. The etched step for the white region was out of range, while for the gray region was 4 μm. In (b), the total etched step was 26 μm after 2.06 hours of etching at 50 °C in 10% KOH at rate of 12.6 μm/hr. Notice the sharp definitions of the pattern edges.

In fig. (4.19), The SEM micrographs show another etching results of different sample etched under similar conditions. The etching rate of this sample was 13.6 μm/hr. In (a), a 100 μm cantilever beam is shown with some curl upward (almost 5 μm). In (b), a close up to this cantilever beam show this curl. In addition to that, the surface roughness is shown. Notice the valleys of non uniform etching around the cantilever region. In (c), a 0.81 μm thick cantilever is shown.

#### **4.6. Optical Switch Fabrication Results**

As mentioned in chapter (3), two techniques were used to fabricate the cantilever optical switch. The first technique was done by using positive PR AZ 4620-E. While the second was done by using the negative PR AZ 5214. In the following sections the experimental results of these techniques will be presented.

#### 4.6.1. Positive PR AZ 4620-E Technique Results

According to the optical microscope observations, the mirrors were covered by 3-4  $\mu\text{m}$  of photoresist, while the upper regions of the mirror's sidewalls weren't covered. This observation was taken after PR development. Fig. (4.20) shows a drawing of these observations.

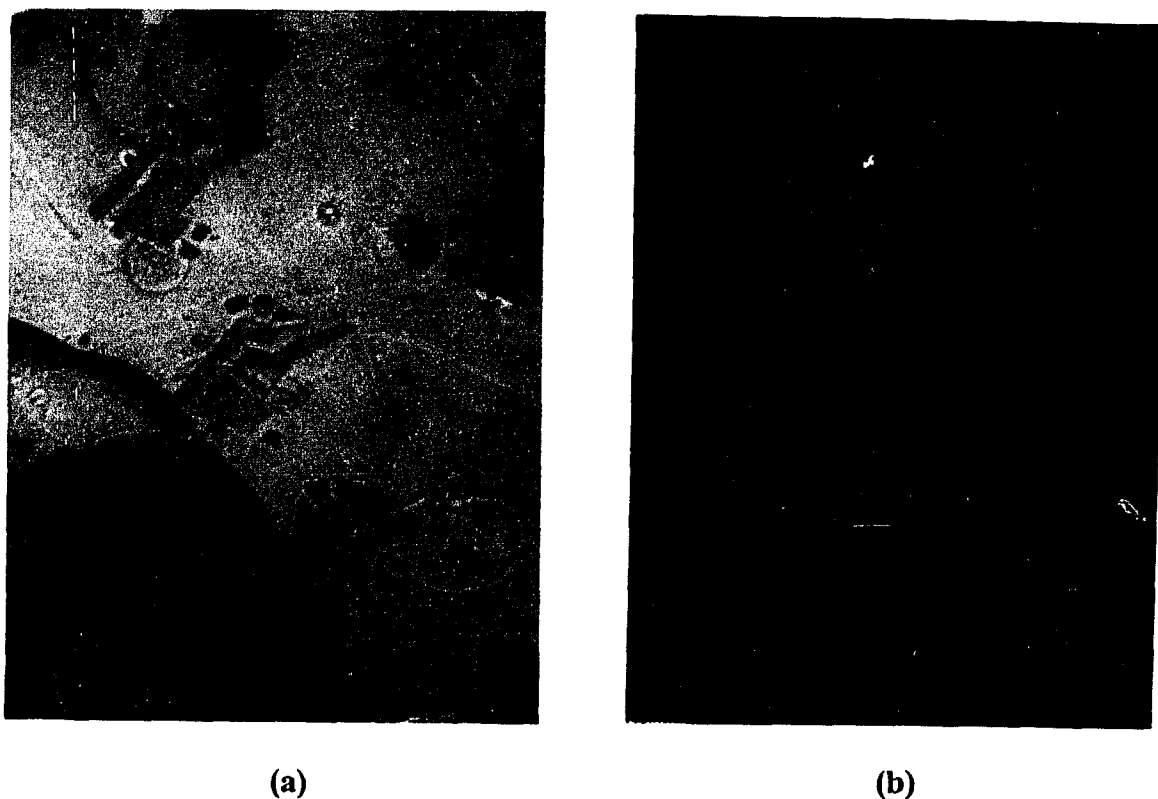


**Figure 4.18** The etching results of a cantilever pattern fabricated by spin on doped glass technology. In (a), notice the white and gray regions with zero and 4  $\mu\text{m}$  etched step respectively. In (b), the etched step was 26  $\mu\text{m}$  after 2.06 hours of etching in 10% KOH at 50  $^{\circ}\text{C}$ . The sharp pattern definition is evident.

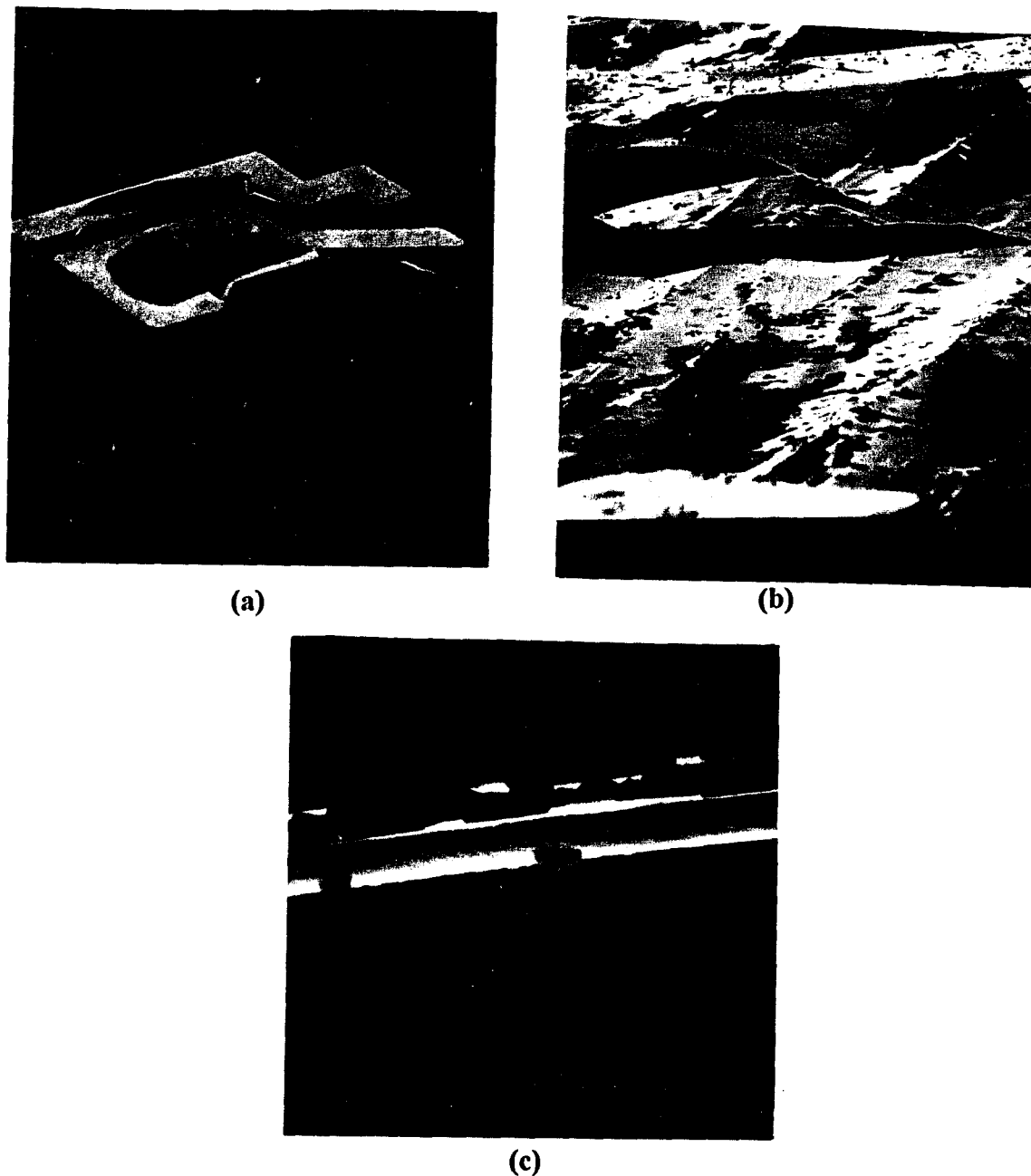


**Figure 4.19** SEM micrographs for a cantilever beam fabricated by SOG. In (a), the top view of 100  $\mu\text{m}$  long cantilever is shown with some curl up. In (b), a micrograph shows the non uniformity of the etched surface beside the curl of the cantilever beam. In (c), the thickness of a cantilever beam fabricated by SOG technology after 2.06 hours of etching in 10% KOH at 50  $^{\circ}\text{C}$  was 0.81  $\mu\text{m}$ .

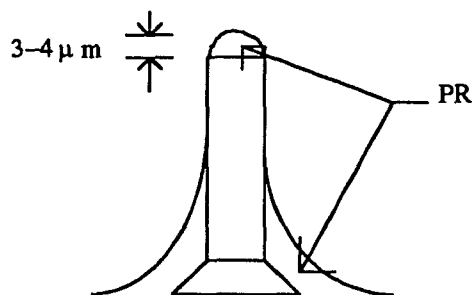


**Figure 4.20** A cross section of the mirror after the spinning and development of the positive PR AZ 4620-E.

Also, after the development of the sample, it was noticed that the photoresist didn't develop completely. About 5-6  $\mu\text{m}$  of PR were left across the entire sample. Fig. (4.21) shows a cross section in the sample after photoresist development.

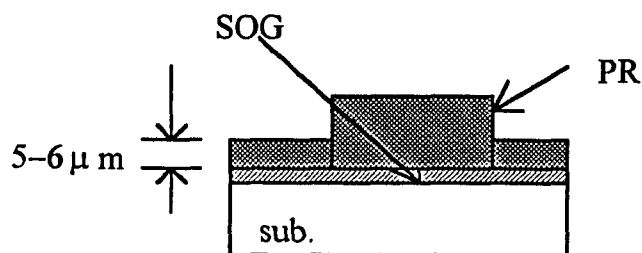


**Fig. 4.21** A cross section shows an incomplete development of the sample processed with cured SOG + PR AZ 4620.

As a result of this incomplete development of the PR, the experiment was terminated.

#### 4.6.2. Negative PR AZ 5214 Technique Results

The SEM micrographs shown in figure (4.22) are for an attempt to fabricate an optical switch by using negative thin PR AZ 5214 to transfer the cantilever pattern to the wafer surface. The total etching time was 75 minutes, which was done in 10% KOH at 50 °C. The etching rate was 13.5  $\mu\text{m/hr}$ . Notice the nonuniformity of the etched surface at the bottom of the cantilever shown in (a). Also, the cantilever wasn't completely free.

Usually, the cantilever beam is free in about one hour. Most of the mirror structure was etched except around the edges and a small portion of the middle. In (b), a close up to the mirror structure shows no change in the thickness of the unetched parts. The thickness of the mirror was  $1.5 \mu\text{m}$  before and after the experiment according to the optical microscope measurements.

Another observation found was the separation of the cantilever beam and the mirror, fig.(4.23). This problem encountered in about 30% of the patter.

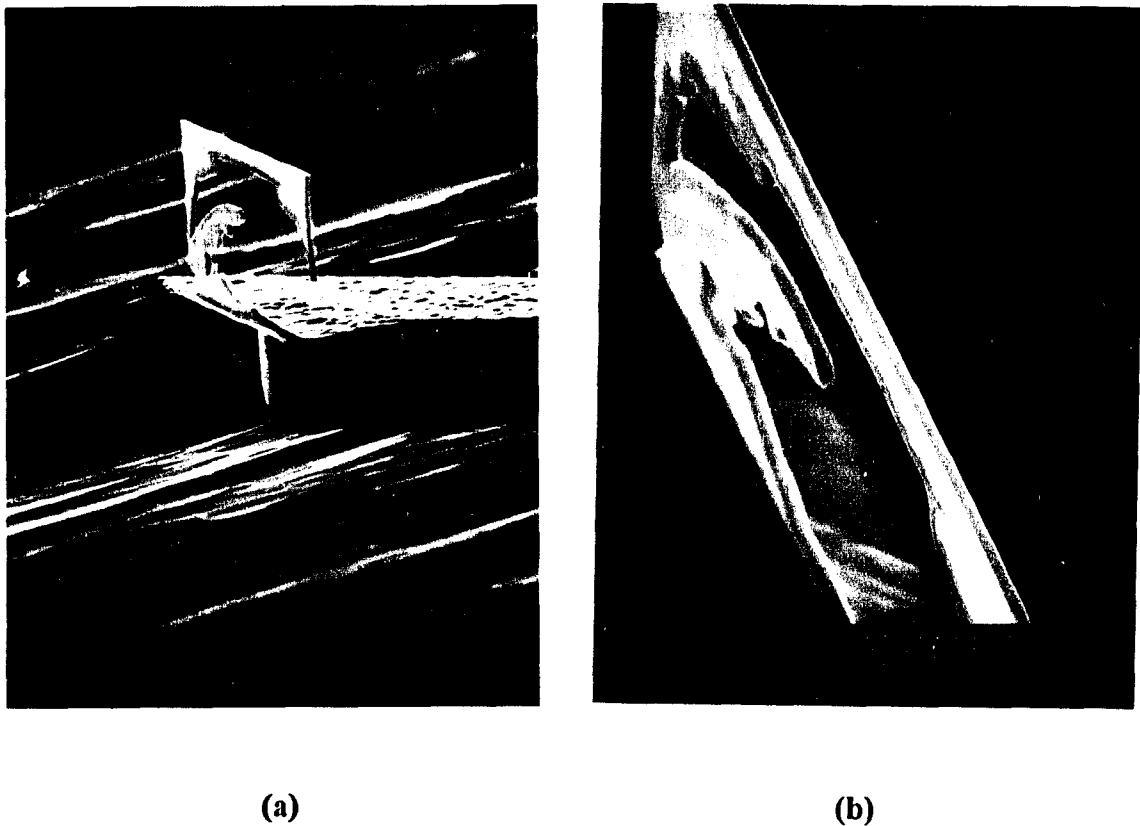


**Figure 4.22** SEM micrographs for optical switch fabrication results which was done by using SOG technology and negative PR AZ 5214. Notice the incomplete etching of Si beneath the cantilever, (a). Also, notice that the unprotected regions of the mirror with SOG was etched. Also, the nonuniformity of etched Si surface. In (b), a close up for the unetched regions shows a uniform mirror thickness.

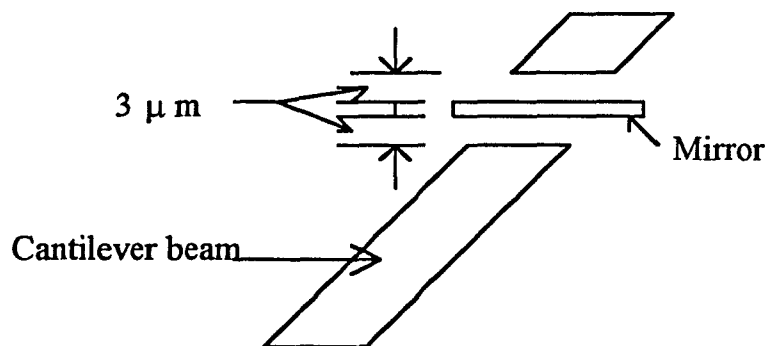


**Fig. 4.23** A graph of the cantilever beam fabricated by thin PR Technique after etching shows the separation of the cantilever beam and the mirror around the mirror base due to proximity effects.

#### 4.7 Surface Smoothing Experimental Results

As mentioned in reference (2), the etching behavior of any surface, i.e. the surface smoothness, will be a function of the area of the surface exposed to the etchants. The smaller the exposed areas, the smoother the surface<sup>(2)</sup>. The design of the cantilever pattern took into account the future the compatibility of integration with other circuits. This results in a huge empty areas between the optical switches. This will cause the etched silicon <110> orientation surface to have linearly textured structures with pyramid shapes. These pyramid shapes are said to be <331> planes, [see fig. (4.1) for the mirror base and fig. (4.6.a) for the SEM micrograph]. Slowing down the etch rates of these planes might help in getting a smoother surfaces.

Isopropyl alcohol was tried for this purpose. In this experiment, the solution composition was :

40% KOH solution + 25% Isopropyl alcohol ;

The experiment was done at  $40^{\circ}\text{C} \pm 2^{\circ}\text{C}$ . The sample had  $2.5\ \mu\text{m}$  thick mirrors with height of  $30\ \mu\text{m}$ . The sample etched for 1 hour. It was observed that the mirror thickness had no change, while its height gained  $2\ \mu\text{m}$ . Also, the sharp peaks of the etched <331> planes became more rounded, but still have the same height. The distance between these peaks increased as shown in fig. (4.24.a,b).

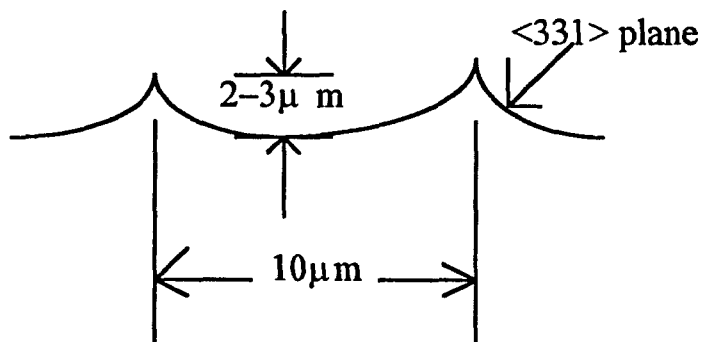


**Figure 4.24.a,** A cross section of a  $\langle 110 \rangle$  Si etched surface shows the surface roughness before using Isopropyl KOH solution.

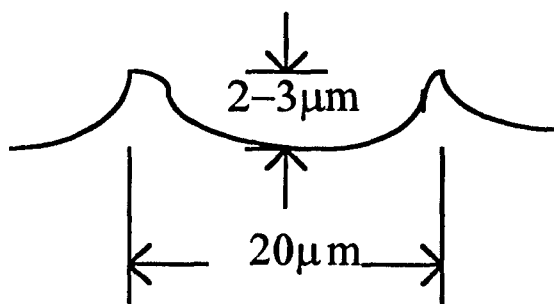


**Figure 4.24.b,** A cross section of the above sample shows the rounded peaks of the  $\langle 331 \rangle$  planes. This sample etched for one hour in Isopropyl KOH solution at  $40^\circ\text{C}$ . Notice the unchanged in the peaks' heights or the distance between them.

## CHAPTER (5)

### DISCUSSION OF EXPERIMENTAL RESULTS

#### 5.1. Introduction

The experimental results in chapter (4) were presented in sections according to the technologies used to introduce the heavily doped etch resistance boron layers. The results of two different methods by which one can fabricate the optical switch and the effect of adding alcohol to the etching solutions were also presented.

These results will be discussed in the same sequence as they were described in chapter (4).

#### 5.2. Heavily Doped Layers Epitaxially Grown

The objective of this experiment was to study the etch resistance of heavily doped boron layers prepared by epitaxial growth.

In the doping profiles shown in fig. (3.4) to (3.6), one can consider the thickness of the region where the doping concentration is  $4 \times 10^{19} \text{ cm}^{-3}$  and higher as flat regions, instead of Gaussian distributions, to estimate The etching rates of these layers. As shown in fig. (3.3) to (3.5), the thicknesses of these regions were, 0.8  $\mu\text{m}$ , 2  $\mu\text{m}$  and 2  $\mu\text{m}$ , respectively. The etching rates measured, as seen in fig. (4.3) to fig. (4.5) were 0.44  $\mu\text{m/hr.}$ , 8  $\mu\text{m/hr}$  and 5  $\mu\text{m/hr}$ , respectively. These results are reasonable if compared with Seidel data<sup>(2)</sup>. His etching rate at a boron concentration of  $4 \times 10^{19}/\text{cm}^3$  determined was 5  $\mu\text{m/hr}$ , but for 60 °C versus 40 °C. Because of the Arrhenious relation between the etch rate and temperature, one would expect the etch rates at 40 °C to be lower than what were measured in this research by a factor of 93%. The difference in crystal orientation <100> for Seidel's experiments versus determined <110> in this work, will provide a factor of 45%. However a factor of about 45% higher



in this research was obtained. This could be due to defects as it is difficult to grow high quality epitaxial layers with high impurity concentrations. The observation of differently colored regions indicative of high defect concentrations. Considering the data published in reference (2), one needs an eleven  $\mu\text{m}$  thick layer of heavily doped boron to be able to form a 1  $\mu\text{m}$  thick cantilever beam, after etching 2 hours in 10% KOH at 50  $^{\circ}\text{C}$  to clear out the region under the cantilever to a depth of 40  $\mu\text{m}$ . This thickness is not achievable by the presently available epitaxial growth technology at SPIRE CORP. Research to improve the epitaxial growth technology would be necessary to make the epi layer approach viable.

### **5.3. Heavily Doped Layers Introduced By Ion Implantation**

#### **5.3.1. $\text{P}^{++}$ Layer Etching**

The first sample received 2 implant doses to raise the boron concentration to  $2 \times 10^{20} \text{cm}^{-3}$  and then was given a standard post implant anneal for 15 minutes at 1000  $^{\circ}\text{C}$ . The sample had a 2.2  $\mu\text{m}$  thick silicon oxide mask. According to computer calculations and based on the boron dosage used, the thickness of the boron layer was 0.83  $\mu\text{m}$ . After removing the oxide mask, the  $\langle 110 \rangle$  silicon sample was etched in 10% KOH at 50  $^{\circ}\text{C}$  for two hours. From fig. (4.6.c), the final cantilever thickness was 0.44  $\mu\text{m}$ . This indicated that the etching rate of the  $\text{p}^{++}$  layer was only 0.0975  $\mu\text{m/hr}$ . The etching rate is approximate because the cantilever beam does not etch from both sides until it is totally free, which took 1 hour [see section (4.4.1)]. Thus the actual etching rate is somewhat higher by a factor of 30% to 50%, see fig. (5.1).

#### **5.3.2. Ion Implantation Masking Effects**

Different type of masks were used against ion implantation to determine the best mask material for that process. The etch rate for  $\langle 110 \rangle$  silicon under the mask is indicated by

the etch rate values calculated from figures (4.8), (4.10), (4.12) and (4.14). It can be seen that, only mask No. 3 was the implant entirely blocked under the mask. Since the etch rate was the expected rate of  $19 \mu\text{m/h}$  <sup>(11)</sup>, while the other samples show slower etch rates which indicate that the masking was incomplete.

Also, the jaggging of the cantilever pattern shown in fig (4.7) and its thin texture at the edge might have contributed to the thick mask tapering effects at the mask edges, so the ions scatter well inside the areas indicated by the mask openings, as shown in fig. (5.2). This effect was not observed for thinner masks sample.

### 5.3.3. Mechanical Stresses Effects Due To High Doping Concentration

As shown in figs (4.6.a) and (4.6.b), cantilever beams tend to curl upward by. This was observed particularly for cantilever beams longer than  $150 \mu\text{m}$ . At this a high with possible incomplete annealing, it is possible that lattice stresses will be generated that could cause curling of the beams. These samples were annealed at  $1000^\circ\text{C}$  for 30 minutes.

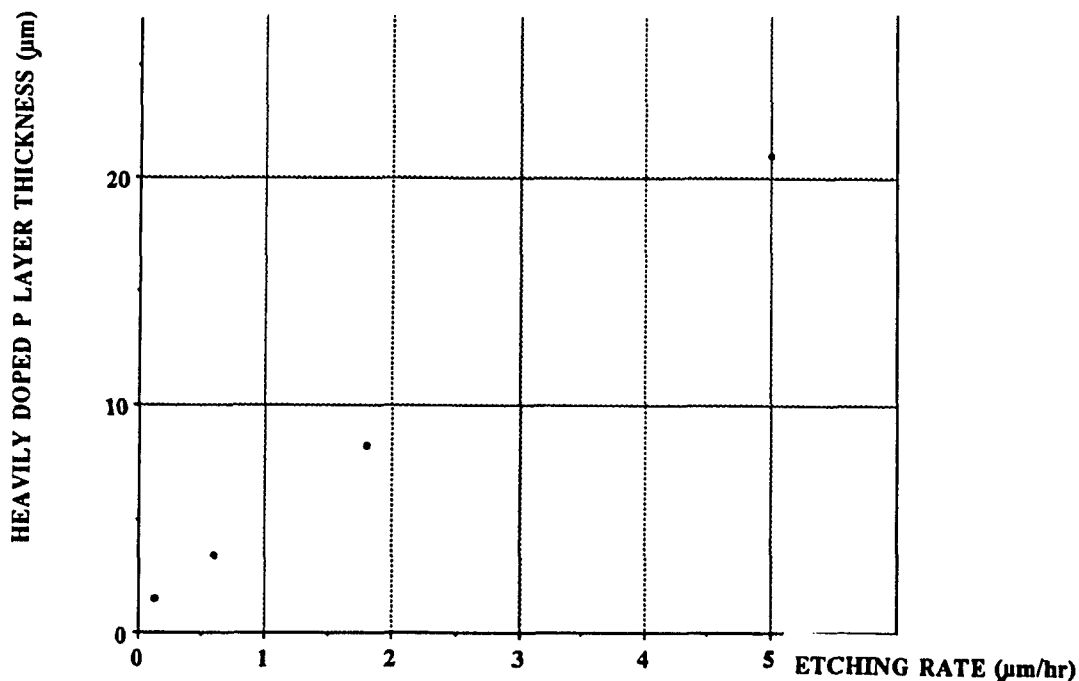
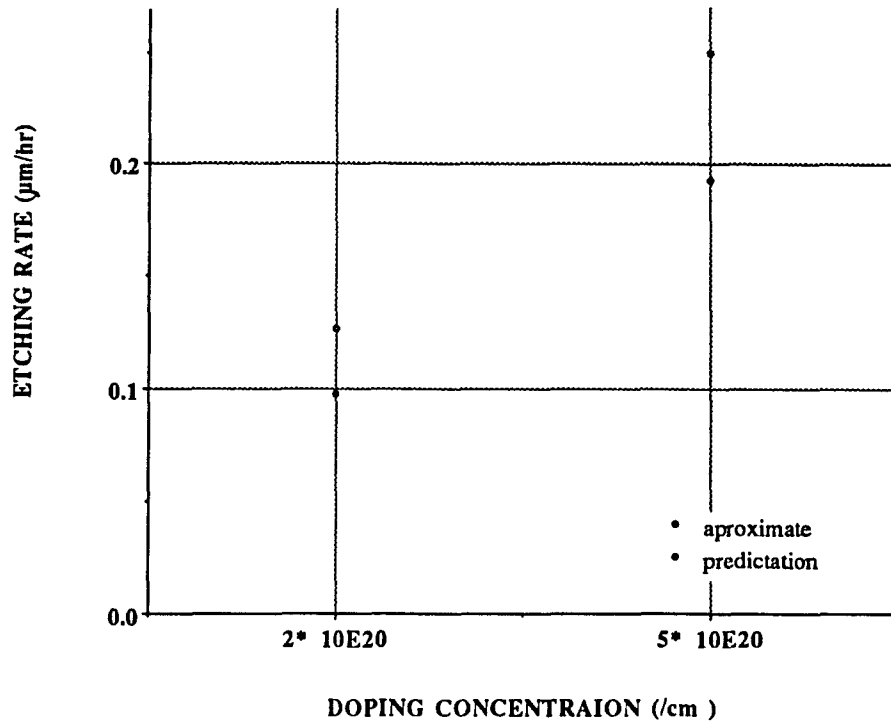
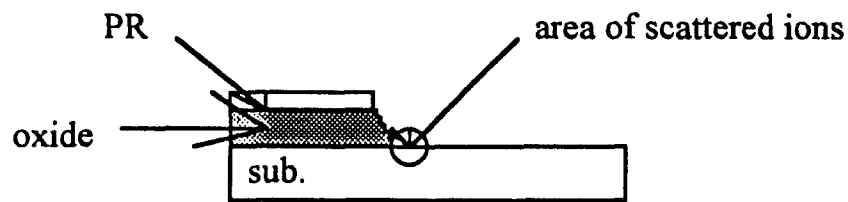


Figure 5.1.a, A graph shows the required thickness of heavily doped layers to fabricate  $1 \mu\text{m}$  thick cantilever beams versus the etch rates of these layers.



**Figure 5.1.b.** A graph shows the measured etch rates of  $p^{++}$  layers at different doping concentrations versus the predicted ones.



**Figure 5.2** A cross section in the oxide + PR mask shows the tapering effects of the mask in ion implantation technique.

Further annealing might reduce the stress. It was mentioned in reference (2), simultaneous codoping with germanium or other element might compensate for these strains and produce stress free cantilever beams (2).

#### 5.3.4. Inward Versus Downward <110> Etching Rates

In fig. (4.16), the inward versus the downward etching rates from the acute angle side of the post is shown. The inward etching rate was half of the downward etch rate. While in fig. (4.17), the inward etch rate from the obtuse angle to the downward rate ratio is shown to be 1:1. This phenomena probably occurs because the atoms at these corners are arranged differently; thus their etching activation energies will differ and the etching rates to be different. This is not a practical problem since the post can be enlarged to compensate for faster inward etching.

#### 5.3.5. Problems Associated With Ion Implantation

The best results of ion implantation experiments were a maximum doping concentration of  $2.5 \times 10^{20} \text{ cm}^{-3}$  in 0.83  $\mu\text{m}$  layer. Since the etching rate of <111> plane is 0.85  $\mu\text{m/hr}$ , using the KOH solution (10% at 50  $^{\circ}\text{C}$ ) that produces the highest etch resistance of heavily doped silicon, the mirror will loose 3.4  $\mu\text{m}$  of its thickness over a period of 2 hours. Thus thickness and doping concentration obtainable by ion implantation, with the available mask, were inadequate for optical switch fabrication. There will be additional mirror thickness lost during the growth of the 2.2  $\mu\text{m}$  thick oxide mask that will be about 1  $\mu\text{m}$  from each side. Thus initially 7.5  $\mu\text{m}$  thick mirrors will be needed to form mirrors with final thicknesses of 2  $\mu\text{m}$ . The mask available for this research could be used to make mirrors of only 2-5  $\mu\text{m}$  thickness.

One could consider increasing the number of doses or even the implant time of ion implantation. However, these were not attractive possibilities because of the expense of the machine time. Also, ion implantation requires annealing out the defects generated by the implant.

## 5.4. Heavily Doped Layers Introduced By Spin On Glass (SOG)

### 5.4.1. Etching Rate Of P<sup>++</sup> Regions And Masking Effects

Results in chapter (4) showed that the p<sup>++</sup> layer thickness was 1.9  $\mu\text{m}$  according to sheet resistance measurements. Fig. (4.19.c) shows that the measured thickness of the cantilever beam was 0.81 $\mu\text{m}$ . This thickness was obtained after 75 minutes of etching in 10% KOH at 50 °C which corresponds to vertical <110> etch rate of 19  $\mu\text{m/hr}$ . Thus the lowest etching rate for the p<sup>++</sup> layer achieved was 0.1926  $\mu\text{m/hr}$  versus the lowest etch rate for an ion implanted layer of 0.0975  $\mu\text{m/hr}$ .

The etching results of a group of samples are shown in fig. (4.18) and (4.19) where the etching rate for the vertical <110> plane was 12.7  $\mu\text{m/hr}$ . These samples etched in 10% KOH at 50 °C. The result is less by more than 30% of the etching results recorded, 19  $\mu\text{m/hr}$  (10). This means that the accelerated boron ions were not entirely blocked from the silicon by the silicon oxide mask. The thickness of the silicon oxide mask was determined by data extrapolated from published industrial results for the diffusivity of boron into SiO<sub>2</sub> at 1100°C. These results do not consider the effects of high boron concentration. In reference (13), it was pointed out that at high doping concentrations,  $> 3 \times 10^{20} \text{ cm}^{-3}$ , the boron will lower the melting temperature of the oxide film. This will form a thin viscous film at the interface between the doped glass and the oxide. The diffusivity of boron atoms will increase through this film. This could explain the nonuniformity of the etched surface shown in fig. (4.22.a). Thus it can be concluded a 5000 Å thickness of SiO<sub>2</sub> was not adequate as a mask against the diffusion of boron with a concentration  $5 \times 10^{20} \text{ cm}^{-3}$ . Similar results (13.6  $\mu\text{m/hr}$ ) for the etching rates under the oxide mask are shown in fig. (4.22). More experiments should be done with different oxide mask thicknesses to determine the best thickness suitable for masking against a boron concentration of  $5 \times 10^{20} \text{ cm}^{-3}$ .

## 5.5. Device Fabrication

Two approaches were used to mask the SOG layer so as to fabricate the optical switch. The first used 40  $\mu\text{m}$  thick photoresist AZ 4620-E. The other approach used a negative thin (1.4  $\mu\text{m}$ ) negative photoresist AZ 5214.

In the following sections a discussion of the results for both techniques will be presented.

### 5.5.1. Positive Thick Photoresist Approach

The first problem encountered using this approach is that full development of the photoresist can be difficult as shown in Fig. (4.21). This problem probably occurred because of the chemical reaction between the SOG and the photoresist. Since the SOG has some organic solvents that may not evaporate during the curing process, the SOG may react with the PR. About 5-6  $\mu\text{m}$  of the PR did not develop. To overcome this problem, one could use reactive ion etching instead of the normal buffered oxide etch, to complete the etching of the photoresist and the SOG layer as pointed out in chapter (3). A drawback of this approach is that the PR covering the top of the mirror is not thick enough, so that at least 2-3  $\mu\text{m}$  of the mirror's top will be etched. This might be solved by using mirrors that have additional height to compensate for the expected etched height. This problem is shown in figure (5.3). Because of these difficulties a more attractive approach was pursued.

### 5.5.2. Negative Thin Photoresist Approach

This procedure of using thin negative photoresist to fabricate the optical switch was described in chapter (3).

The discussion of the results can be by pointing out problems' areas:

- 1) Masking against boron diffusion through the oxide mask as discussed previously in section (5.4);

- 2) Mirror thinning, i.e. etching rate of the  $\langle 111 \rangle$  plane during the formation of the cantilever;
- 3) The separation between the mirror and the cantilever due to proximity effects.

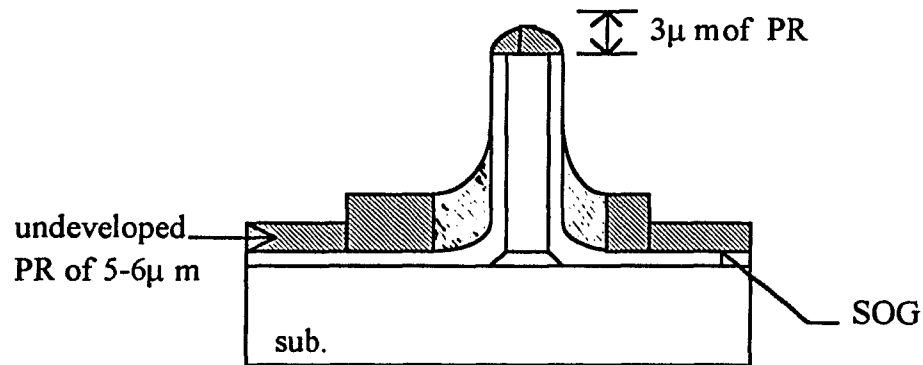


**Figure 5.3** A cross section of a sample in which PR AZ 4620-E used to transfer the cantilever pattern. Notice that the mirror's top is covered by about  $3 \mu\text{m}$  of PR, while the undeveloped parts of the sample are covered by  $5\text{-}6 \mu\text{m}$  of PR. This will result in etching part of the mirror's height in case of using RIE to etch the PR + SOG.

### 5.5.2.1 Mirror Thinning

Using SOG approach, the thinning of the mirror described in sec.(5.3.5) can be solved as by protecting the side walls of the mirror by doped glass. Figures 4.22.a,b show a mirror that was  $1.5 \mu\text{m}$  thick in the beginning of the cantilever fabrication process. It is clear that much of the mirror material had been etched except near the edges. The etching time was 75 minutes. By using an optical microscope, the unetched mirror thickness was still  $1.5 \mu\text{m}$ . This means that the mirror etched at an average rate of  $0.6 \mu\text{m/hr}$  versus the etch rate of undoped  $\langle 111 \rangle$  plane  $0.85 \mu\text{m/hr}$ , as seen in table (2.1). This problem developed because of the vertical surfaces of the mirror were not coated by SOG on one

or both sides. Not coating the mirror was probably the result of putting the SOG on with a speed of 3000 rpm at which the centrifugal force is too high to allow the SOG to stick to the vertical mirror wall.

An approach that will probably work is to spin the SOG on initially at a very low speed and gradually increase the speed after all surfaces are coated to obtain the desired thickness, which will be based on the final speed. The project was terminated at Bellcore before this approach could be tried.

#### 5.5.2.2. Cantilever Beam Separation From The Mirror

Fig. (5.4) shows a comparison between the normal photolithography step needed to transfer the cantilever mask pattern to an oxide mask (a), and the exposure step required if a mirror is on the surface (b). In the first case, a hard contact mode of the mask aligner can be used where  $g$ , the distance between the mask and the sample, can be less than the wavelength of the UV light. While in the second case, the soft contact mode must be used with  $g$  being 32-40  $\mu\text{m}$ .

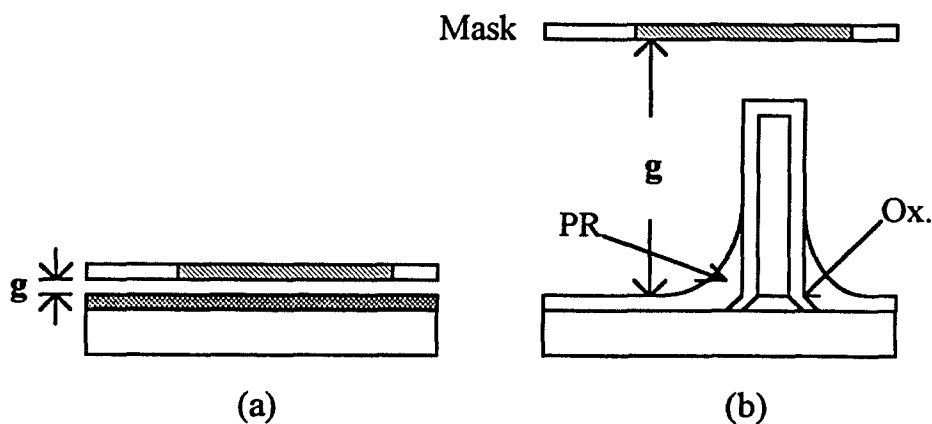


**Figure 5.4** A comparison between exposure step with and without mirrors to transfer the cantilever pattern to the oxide mask using thin negative PR.



In the second case, the printed cantilever pattern will be affected due to the proximity effect. The PR development will be incomplete in the areas around the mirror base which results in PR layer being thicker than  $1.4 \mu\text{m}$ . This in turn will prevent the BOE from etching the oxide mask in these regions preventing the SOG from contacting these regions and thus reducing the boron atoms diffusion around the base of the mirror. After etching the mirror will be separated from cantilever due to this problem, see fig. (4.23). To overcome this problem, one must increase the exposure and the developing times. Experimental work is necessary to find the optimum conditions.

### 5.6. Effect Of Adding Alcohol To The Etchants

Because of the surface roughness at the level of the base of the mirror, after forming the mirror by etching, techniques to smooth the surface before forming the cantilever were investigated.

The results presented in section (4.7) show good agreement with the data published in reference (2) where the etching for the  $\langle 110 \rangle$  planes rate is reduced by 90% by adding 25% of isopropyl alcohol to the etchants.

It was mentioned that the decrease is due to the isopropyl covering the silicon surface, so that the channeling advantage of  $\text{OH}^-$  ions is no longer valid (2). This happens because the etching rate of the  $\langle 110 \rangle$  planes depends on the penetrability of the water molecules into the  $\langle 110 \rangle$  surfaces(2).

Although the desired results of smoothing the  $\langle 331 \rangle$  was demonstrated, more experiments are needed to find the right parameters, i.e. temperature and solution composition, to achieve a smoother surface without affecting the mirror thickness.

## CHAPTER (6)

### SUMMARY AND CONCLUSION

Mirrors of dimensions of  $40 \times 40 \mu\text{m}$ , with thicknesses of  $1.5\text{-}6 \mu\text{m}$  were made using the etch resistance of  $\langle 111 \rangle$  plane and oxide stripes to KOH etchant of concentration 40% at  $50^\circ\text{C}$ . The cantilever beams, which will be used as the moving arms of these mirrors, were fabricated by using the etch resistance of heavily doped boron layers to 10% KOH at  $50^\circ\text{C}$ .

A maximum doping concentration of  $2.5 \times 10^{20} \text{cm}^{-3}$  was achieved in a layer thickness of about  $0.83 \mu\text{m}$  using ion implantation technology. The etching rate of this boron layer as measured was approximately  $0.0975 \mu\text{m/hr}$ . It is recommended to start with a  $7.5 \mu\text{m}$  thick mirror on the mask pattern to fabricate the optical switch. This thickness will compensate the thicknesses that will be lost during oxidation,  $2 \mu\text{m}$ , and  $3.4 \mu\text{m}$  during the final cantilever etching, because of the  $\langle 111 \rangle$  plane not been protected.

The maximum doping concentration achieved using (SOG) technology was  $5 \times 10^{20} \text{cm}^{-3}$  in a  $1.9 \mu\text{m}$  thick layer. After etching 75 minutes in 10% KOH at  $50^\circ\text{C}$ , the etched cantilever thicknesses were  $0.81 \mu\text{m}$ ; thus the boron layer etching rate was  $0.1926 \mu\text{m/hr}$ .

For the SOG technology two techniques were used to fabricate the mirror/cantilever switch. The thick ( $40 \mu\text{m}$ ) positive photoresist method which had a problem of chemical reaction between the photoresist and the spun on glass. The other method, which used a thin ( $1.4 \mu\text{m}$ ) negative photoresist, was more promising. For this method, the spinning speed used for the SOG coating, 3000 rpm, was too high. to allow the SOG to completely wet the mirrors' sidewalls. This caused the etching of the mirror's material as

shown in fig. (4.22). A procedure of slowly increasing the spinning speed from zero to the final value, 3000 rpm, was recommended to overcome this problem. The proximity effect during exposure resulted in separation between the mirror and the cantilever around the base of the mirror. Longer exposure and development times are required to overcome this problem. Also, at higher doping levels ( $> 3 \times 10^{20} \text{ cm}^{-3}$ ), the doped glass reduces the melting point of the oxide mask. This causes the formation of a thin viscous film at the interface between the doped glass and the oxide mask. The diffusivity of boron becomes higher through the oxide mask due to this viscous film. This effect results in low etching rates in "undoped" regions.

Finally, experimental data to find the optimum parameters for complete development of the thick photoresist must be done. Without full development of the photoresist, boron diffusion into unwanted regions outside the cantilever, post, and mirror regions.

## APPENDIX A

A schedule of one dose of ion implantation to introduce a boron layer with doping concentration of  $10^{20} \text{ cm}^{-3}$ .

| Energy (K eV) | Dose ( $\text{cm}^{-2}$ ) |
|---------------|---------------------------|
| 200           | $18 \times 10^{14}$       |
| 150           | $10 \times 10^{14}$       |
| 115           | $9 \times 10^{14}$        |
| 80            | $9 \times 10^{14}$        |
| 50            | $9 \times 10^{14}$        |
| 30            | $6 \times 10^{14}$        |

## BIBLIOGRAPHY

- 1 R. H. Cornely and R. B. Marcus, "Formation of Micromirror by Anisotropic Etching", *Sensors and Actuators A*, 29 (1991), pp. 241-250.
- 2 Seidel, L. Csepregi, A. Heuberger and H. Baumgartel, "Anisotropic Etching of Crystalline Silicon in Alkaline Solutions", I- Orientation Dependence and Behavior of Passivation Layers; II-Influence of Dopants, *electrochem. Soc. Vol. 137, No. 11*, November 1990.
- 3 Peterson, "Silicon as a Mechanical Material", *Proceeding of IEEE*; Vol. 70, No. j, May 1982.
- 4 Kari Gustafsson, "Silicon Micromechanics with Applications in Optical Scanning and Sensing Systems", *Doctoral dissertation - Electronic Dept., Institute of Technology, Upsala Uni., Upsala, Sweden, 1988.*
- 5 Stefan Johnasson, "Micromechanical Properties of Silicon", *Doctoral dissertation from the Faculty of Science, Acta Universitates Upsaliensis, Upsala, Sweden, 1988.*
- 6 Ernest Bassous, "Fabrication of Novel Three Dimensional Microstructures by Anisotropic Etching of <100> and <110> Silicon", *IEEE transaction on ED*, Vol. ED.25. No. 10, Oct. 1978.
- 7 Don L. Kendall, "Vertical Etching of Silicon at Very High Aspect Ratios", *Ann. Rev., material Science* 1979, 9:373.403.
- 8 Csepregi, *Micromechanics: A Silicon Microfabrication Technology*, *Microelectronic Eng.* 3 (1985)221-234, North Holland.
- 9 Runyon, "Crystal Orientation", *Semiconductor Measurement and Instrumentation.*
- 10 Lloyd D. Clark Jr. and David J. Edell, "KOH:H<sub>2</sub>O Etching of <110> Si, SiO<sub>2</sub> and Ta: An Experimental Study"., *IEEE Micro robots and Teleoperator Workshop*, 1987, pp 5-8.
- 11 Personal Communications with Professor Roy H. Cornely.
- 12 Puers and W. Sansen, "Compensation Structures for Convex Corners Micromachining in Si", *Sensors and Actuators A21-A23* (1990) 1036 1041.

- 13 S. M. Sze, *VLSI Technology*, 2 nd. edition, MacGraw-Hill Book Co., 1988, pp. 314-314 and pp. 339-340.